Multiscale and Directional Representations for High-Dimensional Content in Remotely Sensed Data

Daniel Weinberg

Norbert Wiener Center
Department of Mathematics
University of Maryland, College Park

July 27, 2015

Contents of Dissertation and Other Work

- Dissertation
  - **Mathematical preliminaries**
  - **A shearlet application to LIDAR**
  - **Directional superresolution**
  - An aggregation model of phototaxis.
- Other Work
  - Classification of materials from hyperspectral data using Laplacian Eigenmaps (LE) with random projections and approximate SVD.
  - Detection of radioactive material by clustering low-dimensional embeddings of spectra obtained from aerial scans.

In this talk, we present the bolded material.

Directionality

My work is tied together by the fundamental importance of *directionality* in science and mathematics.

- Remote sensing techniques, such as radar, sonar, and LIDAR, involve emitting signals in the form of sound or light. Signals that return to the emitter provide information of the direction of important features.
- It's been hypothesized that the edges of an image are sparsely represented in the human visual cortex. [1]
- Some bacteria orient themselves towards light and form aggregates.
- Dimensionality reduction techniques that require the computation of eigenvectors, such as LE, work by detecting the most significant directions, and hence features, in the data.

[1] D. Field. *Relations between the statistics of natural images and the response properties of cortical cells*. JOSA A. (1987).

Directionality

My work is tied together by the fundamental importance of *directionality* in science and mathematics.

- Remote sensing techniques, such as radar, sonar, and LIDAR, involve emitting signals in the form of sound or light. Signals that return to the emitter provide information of the direction of important features.
- It's been hypothesized that the edges of an image are sparsely represented in the human visual cortex. [1]
- Some bacteria orient themselves towards light and form aggregates.
- Dimensionality reduction techniques that require the computation of eigenvectors, such as LE, work by detecting the most significant directions, and hence features, in the data.

[1] D. Field. *Relations between the statistics of natural images and the response properties of cortical cells*. JOSA A. (1987).

Directionality

My work is tied together by the fundamental importance of *directionality* in science and mathematics.

- Remote sensing techniques, such as radar, sonar, and LIDAR, involve emitting signals in the form of sound or light. Signals that return to the emitter provide information of the direction of important features.
- It's been hypothesized that the edges of an image are sparsely represented in the human visual cortex. [1]
- Some bacteria orient themselves towards light and form aggregates.
- Dimensionality reduction techniques that require the computation of eigenvectors, such as LE, work by detecting the most significant directions, and hence features, in the data.

[1] D. Field. *Relations between the statistics of natural images and the response properties of cortical cells*. JOSA A. (1987).

Directionality

My work is tied together by the fundamental importance of *directionality* in science and mathematics.

- Remote sensing techniques, such as radar, sonar, and LIDAR, involve emitting signals in the form of sound or light. Signals that return to the emitter provide information of the direction of important features.
- It's been hypothesized that the edges of an image are sparsely represented in the human visual cortex. [1]
- Some bacteria orient themselves towards light and form aggregates.
- Dimensionality reduction techniques that require the computation of eigenvectors, such as LE, work by detecting the most significant directions, and hence features, in the data.

[1] D. Field. *Relations between the statistics of natural images and the response properties of cortical cells*. JOSA A. (1987).

Directionality

My work is tied together by the fundamental importance of *directionality* in science and mathematics.

- Remote sensing techniques, such as radar, sonar, and LIDAR, involve emitting signals in the form of sound or light. Signals that return to the emitter provide information of the direction of important features.
- It's been hypothesized that the edges of an image are sparsely represented in the human visual cortex. [1]
- Some bacteria orient themselves towards light and form aggregates.
- Dimensionality reduction techniques that require the computation of eigenvectors, such as LE, work by detecting the most significant directions, and hence features, in the data.

[1] D. Field. *Relations between the statistics of natural images and the response properties of cortical cells*. JOSA A. (1987).

Outline of Talk

Background on Anisotropic Harmonic Analysis

Anisotropic Harmonic Analysis

- Harmonic analysis decomposes signals into simpler elements called *analyzing functions*.
- Classical methods include Fourier series and wavelets. These have proven extremely influential and quite effective for many applications.
- However, they are fundamentally isotropic, meaning they decompose signals without considering how the signal varies directionally.
- Wavelets decompose an image signal with respect to translation and scale. Since the early 2000s, there have been several attempts to incorporate directionality into the wavelet construction.

Anisotropic Harmonic Analysis

- Harmonic analysis decomposes signals into simpler elements called *analyzing functions*.
- Classical methods include Fourier series and wavelets. These have proven extremely influential and quite effective for many applications.
- However, they are fundamentally isotropic, meaning they decompose signals without considering how the signal varies directionally.
- Wavelets decompose an image signal with respect to translation and scale. Since the early 2000s, there have been several attempts to incorporate directionality into the wavelet construction.

Anisotropic Harmonic Analysis

- Harmonic analysis decomposes signals into simpler elements called *analyzing functions*.
- Classical methods include Fourier series and wavelets. These have proven extremely influential and quite effective for many applications.
- However, they are fundamentally isotropic, meaning they decompose signals without considering how the signal varies directionally.
- Wavelets decompose an image signal with respect to translation and scale. Since the early 2000s, there have been several attempts to incorporate directionality into the wavelet construction.

Anisotropic Harmonic Analysis

- Harmonic analysis decomposes signals into simpler elements called *analyzing functions*.
- Classical methods include Fourier series and wavelets. These have proven extremely influential and quite effective for many applications.
- However, they are fundamentally isotropic, meaning they decompose signals without considering how the signal varies directionally.
- Wavelets decompose an image signal with respect to translation and scale. Since the early 2000s, there have been several attempts to incorporate directionality into the wavelet construction.

Anisotropic Harmonic Analysis

- These constructions incorporate directionality in a variety of ways.
- Some of the major constructions include:
  - Ridgelets. [2]
  - Curvelets. [3]
  - Contourlets. [4]
  - Shearlets. [5]
- Wavelets, ridgelets, curvelets, and shearlets are all special cases of the recently introduced $\alpha-$molecules. [6]

[2] E. Candès. *Ridgelets: theory and applications*. PhD thesis. (1998).

[3] D. Donoho and E. Candès. *Curvelets: A surprisingly effective nonadaptive representation for objects with edges*. Curve and Surface Fitting. (1999).

[4] M. Do and M. Vetterli. *Contourlets*. Beyond Wavelets. (2001).

[5] D. Labate, W.-Q. Lim, G. Kutyniok, and G. Weiss. *Sparse multidimensional representation using shearlets*. Proc. SPIE 5914. (2005).

[6] P. Grohs, S. Keiper, G. Kutyniok, and M. Schäfer. $\alpha-$*molecules*. arXiv: 1407.4424 (2014).

Anisotropic Harmonic Analysis

- These constructions incorporate directionality in a variety of ways.
- Some of the major constructions include:
  - Ridgelets. [2]
  - Curvelets. [3]
  - Contourlets. [4]
  - Shearlets. [5]
- Wavelets, ridgelets, curvelets, and shearlets are all special cases of the recently introduced $\alpha-$molecules. [6]

[2] E. Candès. *Ridgelets: theory and applications*. PhD thesis. (1998).

[3] D. Donoho and E. Candès. *Curvelets: A surprisingly effective nonadaptive representation for objects with edges*. Curve and Surface Fitting. (1999).

[4] M. Do and M. Vetterli. *Contourlets*. Beyond Wavelets. (2001).

[5] D. Labate, W.-Q. Lim, G. Kutyniok, and G. Weiss. *Sparse multidimensional representation using shearlets*. Proc. SPIE 5914. (2005).

[6] P. Grohs, S. Keiper, G. Kutyniok, and M. Schäfer. $\alpha-$*molecules*. arXiv: 1407.4421 (2014).

Anisotropic Harmonic Analysis

- These constructions incorporate directionality in a variety of ways.
- Some of the major constructions include:
  - Ridgelets. [2]
  - Curvelets. [3]
  - Contourlets. [4]
  - Shearlets. [5]
- Wavelets, ridgelets, curvelets, and shearlets are all special cases of the recently introduced $\alpha-$molecules. [6]

---

[2] E. Candès. *Ridgelets: theory and applications*. PhD thesis. (1998).

[3] D. Donoho and E. Candès. *Curvelets: A surprisingly effective nonadaptive representation for objects with edges*. Curve and Surface Fitting. (1999).

[4] M. Do and M. Vetterli. *Contourlets*. Beyond Wavelets. (2001).

[5] D. Labate, W.-Q. Lim, G. Kutyniok, and G. Weiss. *Sparse multidimensional representation using shearlets*. Proc. SPIE 5914. (2005).

[6] P. Grohs, S. Keiper, G. Kutyniok, and M. Schäfer. $\alpha-$*molecules*. arXiv: 1407.4424. (2014).

Anisotropic Harmonic Analysis

- A useful model for real images is the class of *cartoon-like images*, $\mathcal{E}^2(\mathbb{R}^2)$.
- Roughly, they are functions that are smooth away from a smooth curve of discontinuity.
- Let $f \in \mathcal{E}^2(\mathbb{R}^2)$ and let f_N be its best N-term approximation with respect to a set of analyzing functions. The optimal asymptotic decay rate of $||f - f_N||_2^2$ is $O(N^{-2}), N \to \infty$, achieved adaptively.
- Up to a log factor, curvelets, contourlets, and shearlets satisfy this optimal decay rate (ridgelets are only optimal for linear boundaries). Hence, these analyzing functions are *essentially optimally sparse* for cartoon-like images. Wavelets can only achieve $O(N^{-1})$. Fourier series are even worse with $O(N^{-1/2})$.
- We focus on shearlets since they have multiple, efficient numerical implementations.

Anisotropic Harmonic Analysis

- A useful model for real images is the class of *cartoon-like images*, $\mathcal{E}^2(\mathbb{R}^2)$.
- Roughly, they are functions that are smooth away from a smooth curve of discontinuity.
- Let $f \in \mathcal{E}^2(\mathbb{R}^2)$ and let f_N be its best N-term approximation with respect to a set of analyzing functions. The optimal asymptotic decay rate of $||f - f_N||_2^2$ is $O(N^{-2}), N \to \infty$, achieved adaptively.
- Up to a log factor, curvelets, contourlets, and shearlets satisfy this optimal decay rate (ridgelets are only optimal for linear boundaries). Hence, these analyzing functions are *essentially optimally sparse* for cartoon-like images. Wavelets can only achieve $O(N^{-1})$. Fourier series are even worse with $O(N^{-1/2})$.
- We focus on shearlets since they have multiple, efficient numerical implementations.

Anisotropic Harmonic Analysis

- A useful model for real images is the class of *cartoon-like images*, $\mathcal{E}^2(\mathbb{R}^2)$.
- Roughly, they are functions that are smooth away from a smooth curve of discontinuity.
- Let $f \in \mathcal{E}^2(\mathbb{R}^2)$ and let f_N be its best N-term approximation with respect to a set of analyzing functions. The optimal asymptotic decay rate of $||f - f_N||_2^2$ is $O(N^{-2}), N \to \infty$, achieved adaptively.
- Up to a log factor, curvelets, contourlets, and shearlets satisfy this optimal decay rate (ridgelets are only optimal for linear boundaries). Hence, these analyzing functions are *essentially optimally sparse* for cartoon-like images. Wavelets can only achieve $O(N^{-1})$. Fourier series are even worse with $O(N^{-1/2})$.
- We focus on shearlets since they have multiple, efficient numerical implementations.

Anisotropic Harmonic Analysis

- A useful model for real images is the class of *cartoon-like images*, $\mathcal{E}^2(\mathbb{R}^2)$.
- Roughly, they are functions that are smooth away from a smooth curve of discontinuity.
- Let $f \in \mathcal{E}^2(\mathbb{R}^2)$ and let f_N be its best N-term approximation with respect to a set of analyzing functions. The optimal asymptotic decay rate of $||f - f_N||_2^2$ is $O(N^{-2}), N \to \infty$, achieved adaptively.
- Up to a log factor, curvelets, contourlets, and shearlets satisfy this optimal decay rate (ridgelets are only optimal for linear boundaries). Hence, these analyzing functions are *essentially optimally sparse* for cartoon-like images. Wavelets can only achieve $O(N^{-1})$. Fourier series are even worse with $O(N^{-1/2})$.
- We focus on shearlets since they have multiple, efficient numerical implementations.

Anisotropic Harmonic Analysis

- A useful model for real images is the class of *cartoon-like images*, $\mathcal{E}^2(\mathbb{R}^2)$.
- Roughly, they are functions that are smooth away from a smooth curve of discontinuity.
- Let $f \in \mathcal{E}^2(\mathbb{R}^2)$ and let f_N be its best N-term approximation with respect to a set of analyzing functions. The optimal asymptotic decay rate of $||f - f_N||_2^2$ is $O(N^{-2}), N \to \infty$, achieved adaptively.
- Up to a log factor, curvelets, contourlets, and shearlets satisfy this optimal decay rate (ridgelets are only optimal for linear boundaries). Hence, these analyzing functions are *essentially optimally sparse* for cartoon-like images. Wavelets can only achieve $O(N^{-1})$. Fourier series are even worse with $O(N^{-1/2})$.
- We focus on shearlets since they have multiple, efficient numerical implementations.

Shearlets

We define the *parabolic scaling matrices*

$$A_a = \begin{pmatrix} a & 0 \\ 0 & a^{1/2} \end{pmatrix}, \qquad a > 0$$

and the *shearing matrices*

$$S_s = \begin{pmatrix} 1 & s \\ 0 & 1 \end{pmatrix}, \qquad s \in \mathbb{R}.$$

Also, let D_M be the dilation operator defined by

$$D_M \psi = |\det M|^{-1/2} \psi(M^{-1} \cdot), \qquad M \in GL_2(\mathbb{R})$$

and T_t the translation operator defined by

$$T_t \psi = \psi(\cdot - t), \qquad t \in \mathbb{R}^2.$$

Shearlets

We define the *parabolic scaling matrices*

$$A_a = \begin{pmatrix} a & 0 \\ 0 & a^{1/2} \end{pmatrix}, \qquad a > 0$$

and the *shearing matrices*

$$S_s = \begin{pmatrix} 1 & s \\ 0 & 1 \end{pmatrix}, \qquad s \in \mathbb{R}.$$

Also, let D_M be the dilation operator defined by

$$D_M \psi = |\det M|^{-1/2} \psi(M^{-1} \cdot), \qquad M \in GL_2(\mathbb{R})$$

and T_t the translation operator defined by

$$T_t \psi = \psi(\cdot - t), \qquad t \in \mathbb{R}^2.$$

Shearlets

Definition

Let $\psi \in L^2(\mathbb{R}^2)$. The *Continuous Shearlet Transform* of $f \in L^2(\mathbb{R}^2)$ is

$$f \mapsto \mathscr{SH}_\psi f(a, s, t) = \langle f, T_t D_{A_a} D_{S_s} \psi \rangle, a > 0, s \in \mathbb{R}, t \in \mathbb{R}^2.$$

- Parabolic scaling allows for directional sensitivity.
- Shearing allows us to change this direction.
- By carefully choosing ψ and discretizing the parameter space, we can decompose $f \in L^2(\mathbb{R}^2)$ into a Parseval frame.

Shearlets

Definition

Let $\psi \in L^2(\mathbb{R}^2)$. The *Continuous Shearlet Transform* of $f \in L^2(\mathbb{R}^2)$ is

$$f \mapsto \mathscr{SH}_\psi f(a, s, t) = \langle f, T_t D_{A_a} D_{S_s} \psi \rangle, a > 0, s \in \mathbb{R}, t \in \mathbb{R}^2.$$

- Parabolic scaling allows for directional sensitivity.
- Shearing allows us to change this direction.
- By carefully choosing ψ and discretizing the parameter space, we can decompose $f \in L^2(\mathbb{R}^2)$ into a Parseval frame.

Shearlets

Definition

Let $\psi \in L^2(\mathbb{R}^2)$. The *Continuous Shearlet Transform* of $f \in L^2(\mathbb{R}^2)$ is

$$f \mapsto \mathscr{SH}_\psi f(a, s, t) = \langle f, T_t D_{A_a} D_{S_s} \psi \rangle, a > 0, s \in \mathbb{R}, t \in \mathbb{R}^2.$$

- Parabolic scaling allows for directional sensitivity.
- Shearing allows us to change this direction.
- By carefully choosing ψ and discretizing the parameter space, we can decompose $f \in L^2(\mathbb{R}^2)$ into a Parseval frame.

Shearlets

Definition

Let $\psi \in L^2(\mathbb{R}^2)$. The *Continuous Shearlet Transform* of $f \in L^2(\mathbb{R}^2)$ is

$$f \mapsto \mathscr{SH}_\psi f(a, s, t) = \langle f, T_t D_{A_a} D_{S_s} \psi \rangle, a > 0, s \in \mathbb{R}, t \in \mathbb{R}^2.$$

- Parabolic scaling allows for directional sensitivity.
- Shearing allows us to change this direction.
- By carefully choosing ψ and discretizing the parameter space, we can decompose $f \in L^2(\mathbb{R}^2)$ into a Parseval frame.

Shearlets

- It's generally assumed that $\hat{\psi}$ splits as $\hat{\psi}(\xi_1, \xi_2) = \hat{\psi}_1(\xi_1)\hat{\psi}_2(\xi_2/\xi_1)$.
- The basic shearlet ψ is only used in a *horizontal cone*, while the reflection of ψ across the line $\xi_2 = \xi_1$ is used in a *vertical cone*. A scaling function ϕ is used for the low-pass region. This construction is known as *cone-adapted* shearlets.

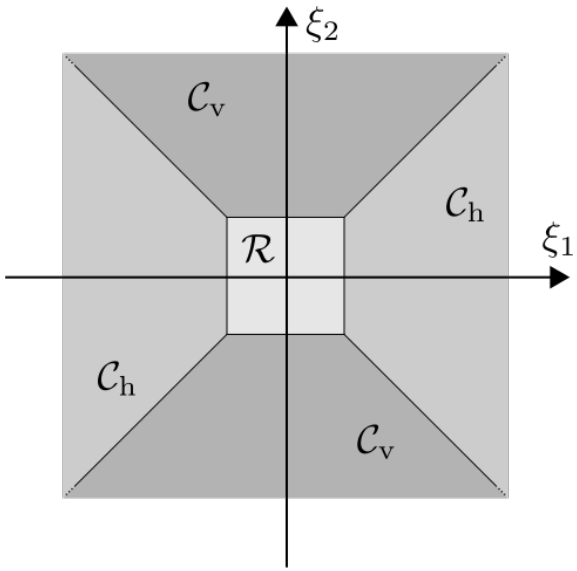

Figure: Frequency tiling for cone-adapted shearlets.[7]

[7] G. Kutyniok and D. Labate, eds. *Shearlets: Multiscale analysis for multivariate data.* Birkhäuser. (2012).

Shearlet Implementations

- Shearlets have several efficient numerical implementations in MATLAB that are freely available.
  - 2D Shearlet Toolbox (Easley, Labate, and Lim). [8]
  - Shearlab (Kutyniok, Shahram, Zhuang et al.). [9]
  - Fast Finite Shearlet Transform (Häuser and Steidl).[10]
- We used the last option (FFST) here, which is in many ways the most intuitive of the implementations.

[8] http://www.math.uh.edu/~dlabate/software.html
[9] http://www.shearlab.org/
[10] http://www.mathematik.uni-kl.de/imagepro/software/ffst/

Shearlet Implementations

- Shearlets have several efficient numerical implementations in MATLAB that are freely available.
  - 2D Shearlet Toolbox (Easley, Labate, and Lim). [8]
  - Shearlab (Kutyniok, Shahram, Zhuang et al.). [9]
  - Fast Finite Shearlet Transform (Häuser and Steidl).[10]
- We used the last option (FFST) here, which is in many ways the most intuitive of the implementations.

[8] http://www.math.uh.edu/~dlabate/software.html
[9] http://www.shearlab.org/
[10] http://www.mathematik.uni-kl.de/imagepro/software/ffst/

Fast Finite Shearlet Transform (FFST)

- Consider an $M \times N$ image. Define $j_0 := \lfloor \log_2 \max\{M, N\} \rfloor$. We discretize the parameters as follows:

$$a_j := 2^{-2j} = \frac{1}{4^j}, \qquad j = 0, \ldots, j_0 - 1,$$

$$s_{j,k} := k2^{-j}, \qquad -2^j \leq k \leq 2^j,$$

$$t_m := \left(\frac{m_1}{M}, \frac{m_2}{N} \right), \quad m_1 = 0, \ldots, M-1, \; m_2 = 0, \ldots, N-1.$$

- Note that the shears vary from -1 to 1. To fill out the remaining directions, we also shear with respect to the y-axis.
- Shearlets whose supports overlap are "glued" together.
- The transform is computed through the $2D$ FFT and iFFT.

Fast Finite Shearlet Transform (FFST)

- Consider an $M \times N$ image. Define $j_0 := \lfloor \log_2 \max\{M, N\} \rfloor$. We discretize the parameters as follows:

$$a_j := 2^{-2j} = \frac{1}{4^j}, \qquad j = 0, \ldots, j_0 - 1,$$

$$s_{j,k} := k2^{-j}, \qquad -2^j \leq k \leq 2^j,$$

$$t_m := \left(\frac{m_1}{M}, \frac{m_2}{N} \right), \quad m_1 = 0, \ldots, M-1, \; m_2 = 0, \ldots, N-1.$$

- Note that the shears vary from -1 to 1. To fill out the remaining directions, we also shear with respect to the y-axis.
- Shearlets whose supports overlap are "glued" together.
- The transform is computed through the $2D$ FFT and iFFT.

Fast Finite Shearlet Transform

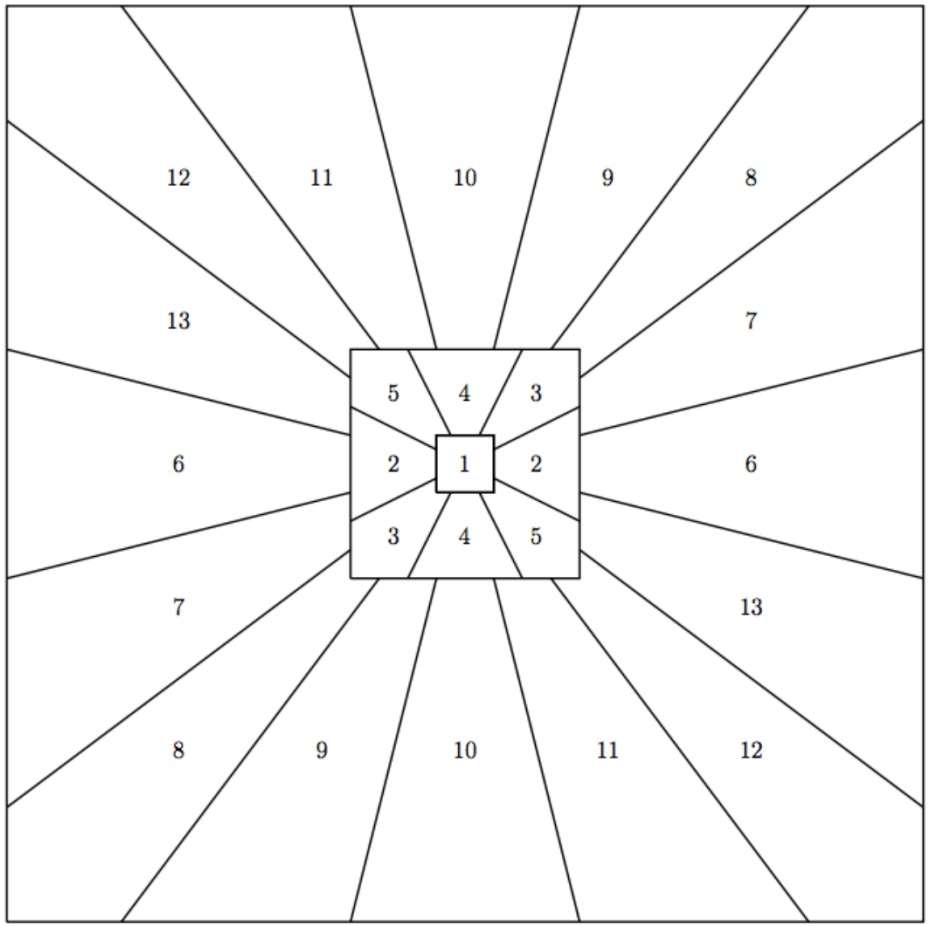

Figure: Frequency tiling for FFST.[11]

[11] S. Häuser and G. Steidl. *Fast finite shearlet transform: a tutorial*. arXiv:1202.1773. (2014).

Fast Finite Shearlet Transform

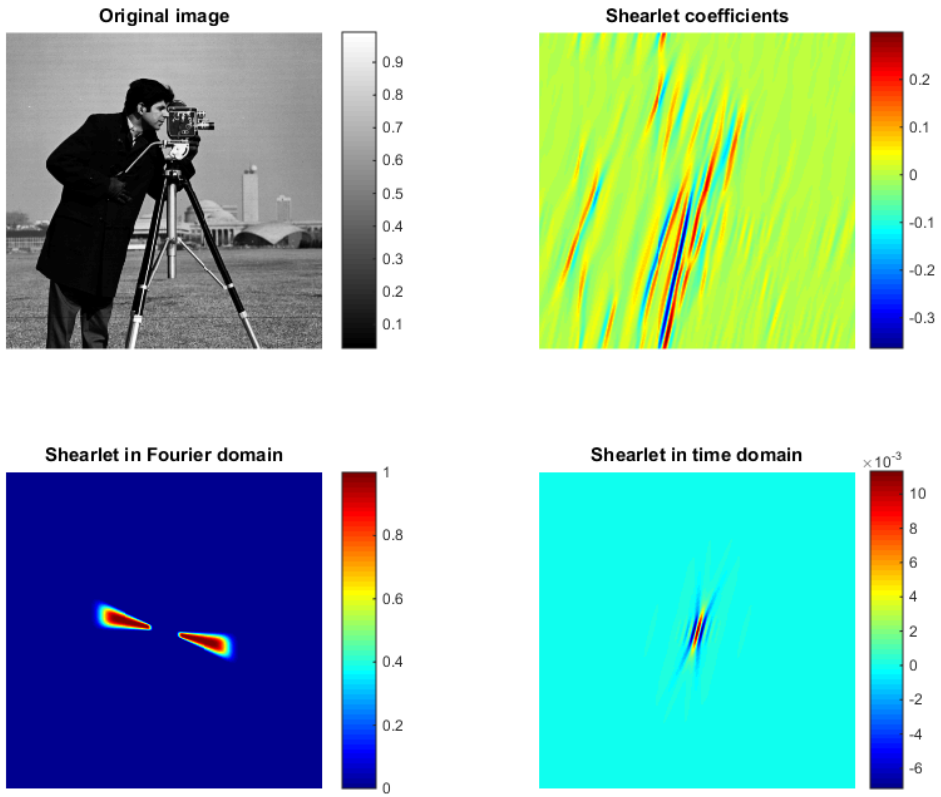

Figure: Demonstration of output from the FFST on the cameraman image. The shearlet coefficients are from scale 3 (out of 4) in the direction of slope 4.

How Well Can the FFST Resolve Directions?

We can prove that the direction of the shearlet coefficient of maximum magnitude determines the direction, at least in the ideal case.

Theorem

Let $f(x) = H_{y>rx}$ be a 2D Heaviside function and assume WLOG that $|r| \leq 1$. Fix a scale j and position m. Then the shearlet coefficient of the FFST $\mathcal{SH}(f)(j,k,m)$ is only nonzero for at most two consecutive values of the shearing parameter k. The value of k that maximizes $|\mathcal{SH}(f)(j,k,m)|$ satisfies

$$\left|s_{j,k} - r\right| < \frac{1}{2^j}.$$

Furthermore, for this k, $s_{j,k}$ is closest to r over all k.

Sketch of Proof

- We first show by direct computation that $\int_{\mathbb{R}} \hat{\psi}(-r\omega, \omega) d\omega = \int_{\mathbb{R}} \psi(x, rx) dx$ for all $\psi \in S(\mathbb{R}^2), r \in \mathbb{R}$.
- Since $\frac{\partial}{\partial y} H_{y>rx} = \delta_{y-rx}$, $\widehat{H_{y>rx}} = \frac{1}{2\pi i \omega_2} \widehat{\delta_{y-rx}}$.
- Using the above, $\langle \widehat{\delta_{y-rx}}, \hat{\psi} \rangle = \int_{\mathbb{R}} \hat{\psi}(-r\omega, \omega) d\omega, \qquad \hat{\psi} \in C_c^\infty(\mathbb{R}^2)$.
- We compute

$$\begin{aligned} \mathcal{SH}(f)(j,k,m) &= \langle f, \psi_{jkm} \rangle \\ &= \langle \hat{f}, \hat{\psi}_{jkm} \rangle \\ &= \int_{\mathbb{R}^2} \frac{1}{2\pi i \omega_2} \widehat{\delta_{y-rx}}(\omega_1, \omega_2) \hat{\psi}_{jkm}(\omega_1, \omega_2) d\omega_1 d\omega_2 \\ &= \frac{1}{2\pi i} \int_{\mathbb{R}} \frac{1}{\omega_2} \hat{\psi}_{jkm}(-r\omega_2, \omega_2) d\omega_2. \end{aligned}$$

Sketch of Proof

- We first show by direct computation that $\int_{\mathbb{R}} \hat{\psi}(-r\omega, \omega) d\omega = \int_{\mathbb{R}} \psi(x, rx) dx$ for all $\psi \in S(\mathbb{R}^2), r \in \mathbb{R}$.
- Since $\frac{\partial}{\partial y} H_{y>rx} = \delta_{y-rx}$, $\widehat{H_{y>rx}} = \frac{1}{2\pi i \omega_2} \widehat{\delta_{y-rx}}$.
- Using the above, $\langle \widehat{\delta_{y-rx}}, \hat{\psi} \rangle = \int_{\mathbb{R}} \hat{\psi}(-r\omega, \omega) d\omega, \qquad \hat{\psi} \in C_c^\infty(\mathbb{R}^2)$.
- We compute

$$\begin{aligned} \mathcal{SH}(f)(j,k,m) &= \langle f, \psi_{jkm} \rangle \\ &= \langle \hat{f}, \hat{\psi}_{jkm} \rangle \\ &= \int_{\mathbb{R}^2} \frac{1}{2\pi i \omega_2} \widehat{\delta_{y-rx}}(\omega_1, \omega_2) \hat{\psi}_{jkm}(\omega_1, \omega_2) d\omega_1 d\omega_2 \\ &= \frac{1}{2\pi i} \int_{\mathbb{R}} \frac{1}{\omega_2} \hat{\psi}_{jkm}(-r\omega_2, \omega_2) d\omega_2. \end{aligned}$$

Sketch of Proof

- We first show by direct computation that $\int_{\mathbb{R}} \hat{\psi}(-r\omega, \omega) d\omega = \int_{\mathbb{R}} \psi(x, rx) dx$ for all $\psi \in S(\mathbb{R}^2), r \in \mathbb{R}$.
- Since $\frac{\partial}{\partial y} H_{y>rx} = \delta_{y-rx}$, $\widehat{H_{y>rx}} = \frac{1}{2\pi i \omega_2} \widehat{\delta_{y-rx}}$.
- Using the above, $\langle \widehat{\delta_{y-rx}}, \hat{\psi} \rangle = \int_{\mathbb{R}} \hat{\psi}(-r\omega, \omega) d\omega, \qquad \hat{\psi} \in C_c^\infty(\mathbb{R}^2)$.
- We compute

$$\begin{aligned} \mathcal{SH}(f)(j,k,m) &= \langle f, \psi_{jkm} \rangle \\ &= \langle \hat{f}, \hat{\psi}_{jkm} \rangle \\ &= \int_{\mathbb{R}^2} \frac{1}{2\pi i \omega_2} \widehat{\delta_{y-rx}}(\omega_1, \omega_2) \hat{\psi}_{jkm}(\omega_1, \omega_2) d\omega_1 d\omega_2 \\ &= \frac{1}{2\pi i} \int_{\mathbb{R}} \frac{1}{\omega_2} \hat{\psi}_{jkm}(-r\omega_2, \omega_2) d\omega_2. \end{aligned}$$

Sketch of Proof

- We first show by direct computation that $\int_{\mathbb{R}} \hat{\psi}(-r\omega, \omega) d\omega = \int_{\mathbb{R}} \psi(x, rx) dx$ for all $\psi \in S(\mathbb{R}^2), r \in \mathbb{R}$.
- Since $\frac{\partial}{\partial y} H_{y>rx} = \delta_{y-rx}$, $\widehat{H_{y>rx}} = \frac{1}{2\pi i \omega_2} \widehat{\delta_{y-rx}}$.
- Using the above, $\langle \widehat{\delta_{y-rx}}, \hat{\psi} \rangle = \int_{\mathbb{R}} \hat{\psi}(-r\omega, \omega) d\omega, \qquad \hat{\psi} \in C_c^\infty(\mathbb{R}^2)$.
- We compute

$$\begin{aligned}
\mathcal{SH}(f)(j,k,m) &= \langle f, \psi_{jkm} \rangle \\
&= \langle \hat{f}, \hat{\psi}_{jkm} \rangle \\
&= \int_{\mathbb{R}^2} \frac{1}{2\pi i \omega_2} \widehat{\delta_{y-rx}}(\omega_1, \omega_2) \hat{\psi}_{jkm}(\omega_1, \omega_2) d\omega_1 d\omega_2 \\
&= \frac{1}{2\pi i} \int_{\mathbb{R}} \frac{1}{\omega_2} \hat{\psi}_{jkm}(-r\omega_2, \omega_2) d\omega_2.
\end{aligned}$$

Sketch of Proof

- By the way $\hat{\psi}$ decomposes,

$$\hat{\psi}_{jkm}(-r\omega_2, \omega_2) = \hat{\psi}_1(4^{-j}\omega_2)\hat{\psi}_2(-2^j r + k)\exp(-2\pi i(-r\omega_2 m_1/M + \omega_2 m_2/N)).$$

- Since k only appears in $\hat{\psi}_2(-2^j r + k)$, we examine that term separately.
- By assumption, $\hat{\psi}_2$ is a positive, smooth function supported on $[-1, 1]$ that is strictly increasing on $[-1, 0]$ and decreasing on $[0, 1]$.
- Hence, to obtain a nonzero shearlet coefficient, we must have $|-2^j r + k| < 1$ or $|s_{j,k} - r| < 1/2^j$.
- The shearlet slopes differ by $1/2^j$, so this can only occur at most twice.
- The coefficient is maximized when $-2^j r + k$ is closest to 0, that is, when $s_{j,k}$ is closest to r.

Sketch of Proof

- By the way $\hat{\psi}$ decomposes,

$$\hat{\psi}_{jkm}(-r\omega_2, \omega_2) = \hat{\psi}_1(4^{-j}\omega_2)\hat{\psi}_2(-2^j r + k)\exp(-2\pi i(-r\omega_2 m_1/M + \omega_2 m_2/N)).$$

- Since k only appears in $\hat{\psi}_2(-2^j r + k)$, we examine that term separately.
- By assumption, $\hat{\psi}_2$ is a positive, smooth function supported on $[-1, 1]$ that is strictly increasing on $[-1, 0]$ and decreasing on $[0, 1]$.
- Hence, to obtain a nonzero shearlet coefficient, we must have $|-2^j r + k| < 1$ or $|s_{j,k} - r| < 1/2^j$.
- The shearlet slopes differ by $1/2^j$, so this can only occur at most twice.
- The coefficient is maximized when $-2^j r + k$ is closest to 0, that is, when $s_{j,k}$ is closest to r.

Sketch of Proof

- By the way $\hat{\psi}$ decomposes,

$$\hat{\psi}_{jkm}(-r\omega_2, \omega_2) = \hat{\psi}_1(4^{-j}\omega_2)\hat{\psi}_2(-2^j r + k)\exp(-2\pi i(-r\omega_2 m_1/M + \omega_2 m_2/N)).$$

- Since k only appears in $\hat{\psi}_2(-2^j r + k)$, we examine that term separately.
- By assumption, $\hat{\psi}_2$ is a positive, smooth function supported on $[-1, 1]$ that is strictly increasing on $[-1, 0]$ and decreasing on $[0, 1]$.
- Hence, to obtain a nonzero shearlet coefficient, we must have $|-2^j r + k| < 1$ or $|s_{j,k} - r| < 1/2^j$.
- The shearlet slopes differ by $1/2^j$, so this can only occur at most twice.
- The coefficient is maximized when $-2^j r + k$ is closest to 0, that is, when $s_{j,k}$ is closest to r.

Sketch of Proof

- By the way $\hat{\psi}$ decomposes,

$$\hat{\psi}_{jkm}(-r\omega_2, \omega_2) = \hat{\psi}_1(4^{-j}\omega_2)\hat{\psi}_2(-2^j r + k)\exp(-2\pi i(-r\omega_2 m_1/M + \omega_2 m_2/N)).$$

- Since k only appears in $\hat{\psi}_2(-2^j r + k)$, we examine that term separately.
- By assumption, $\hat{\psi}_2$ is a positive, smooth function supported on $[-1, 1]$ that is strictly increasing on $[-1, 0]$ and decreasing on $[0, 1]$.
- Hence, to obtain a nonzero shearlet coefficient, we must have $|-2^j r + k| < 1$ or $|s_{j,k} - r| < 1/2^j$.
- The shearlet slopes differ by $1/2^j$, so this can only occur at most twice.
- The coefficient is maximized when $-2^j r + k$ is closest to 0, that is, when $s_{j,k}$ is closest to r.

Sketch of Proof

- By the way $\hat{\psi}$ decomposes,

$$\hat{\psi}_{jkm}(-r\omega_2, \omega_2) = \hat{\psi}_1(4^{-j}\omega_2)\hat{\psi}_2(-2^j r + k)\exp(-2\pi i(-r\omega_2 m_1/M + \omega_2 m_2/N)).$$

- Since k only appears in $\hat{\psi}_2(-2^j r + k)$, we examine that term separately.
- By assumption, $\hat{\psi}_2$ is a positive, smooth function supported on $[-1, 1]$ that is strictly increasing on $[-1, 0]$ and decreasing on $[0, 1]$.
- Hence, to obtain a nonzero shearlet coefficient, we must have $|-2^j r + k| < 1$ or $|s_{j,k} - r| < 1/2^j$.
- The shearlet slopes differ by $1/2^j$, so this can only occur at most twice.
- The coefficient is maximized when $-2^j r + k$ is closest to 0, that is, when $s_{j,k}$ is closest to r.

Sketch of Proof

- By the way $\hat{\psi}$ decomposes,

$$\hat{\psi}_{jkm}(-r\omega_2, \omega_2) = \hat{\psi}_1(4^{-j}\omega_2)\hat{\psi}_2(-2^j r + k)\exp(-2\pi i(-r\omega_2 m_1/M + \omega_2 m_2/N)).$$

- Since k only appears in $\hat{\psi}_2(-2^j r + k)$, we examine that term separately.
- By assumption, $\hat{\psi}_2$ is a positive, smooth function supported on $[-1, 1]$ that is strictly increasing on $[-1, 0]$ and decreasing on $[0, 1]$.
- Hence, to obtain a nonzero shearlet coefficient, we must have $|-2^j r + k| < 1$ or $|s_{j,k} - r| < 1/2^j$.
- The shearlet slopes differ by $1/2^j$, so this can only occur at most twice.
- The coefficient is maximized when $-2^j r + k$ is closest to 0, that is, when $s_{j,k}$ is closest to r.

Directional Superresolution

What is Superresolution?

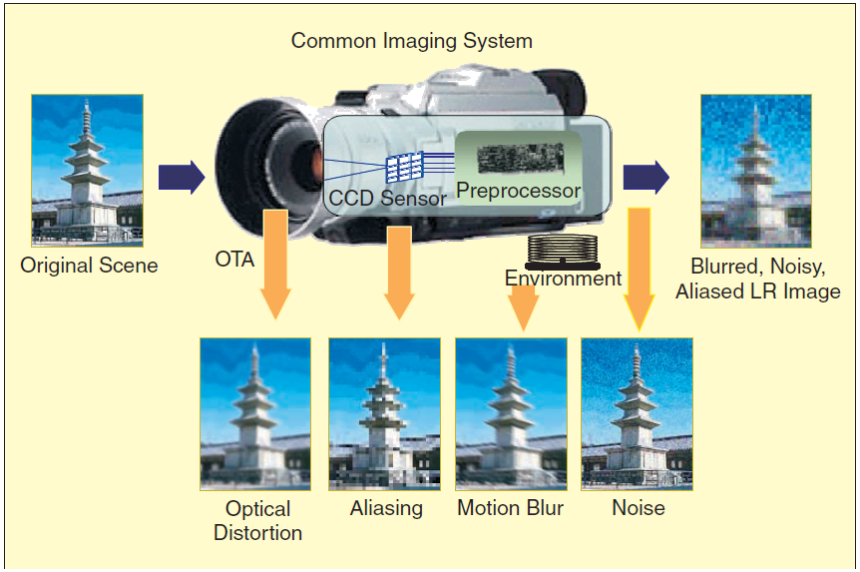

- Superresolution (SR) is the problem of improving the resolution of an image, without introducing artifacts.
- All sensors have a diffraction limit, which restricts resolving power.
- Decreasing pixel size improves resolution, but has the drawback of also decreasing light, leading to shot noise. [12]
- Undersampling leads to aliasing, causing the image to appear blocky.

[12] S. Park, M. Park, and M. Kang. *Super-resolution image reconstruction: a technical overview.* IEEE Signal Processing Magazine 20.3 (2003):21-36.

What is Superresolution?

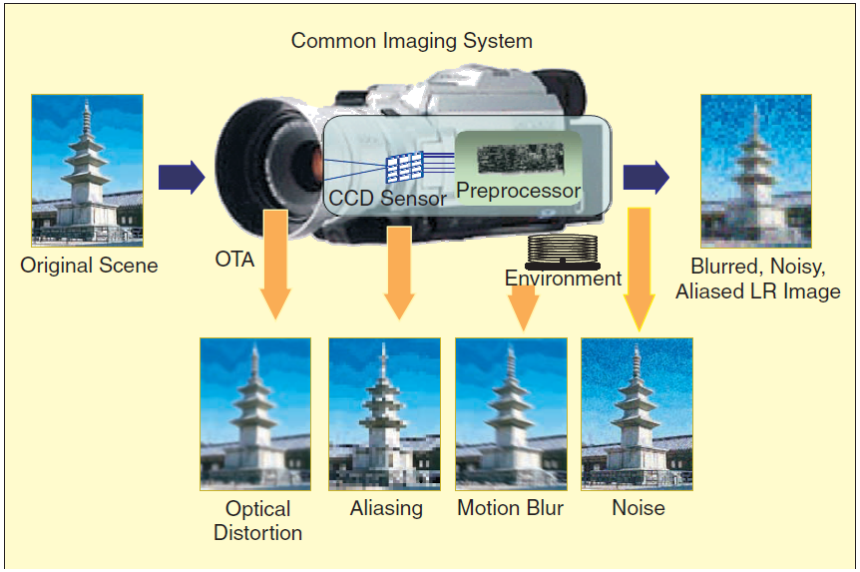

- Superresolution (SR) is the problem of improving the resolution of an image, without introducing artifacts.
- All sensors have a diffraction limit, which restricts resolving power.
- Decreasing pixel size improves resolution, but has the drawback of also decreasing light, leading to shot noise. [12]
- Undersampling leads to aliasing, causing the image to appear blocky.

[12] S. Park, M. Park, and M. Kang. *Super-resolution image reconstruction: a technical overview.* IEEE Signal Processing Magazine 20.3 (2003):21-36.

What is Superresolution?

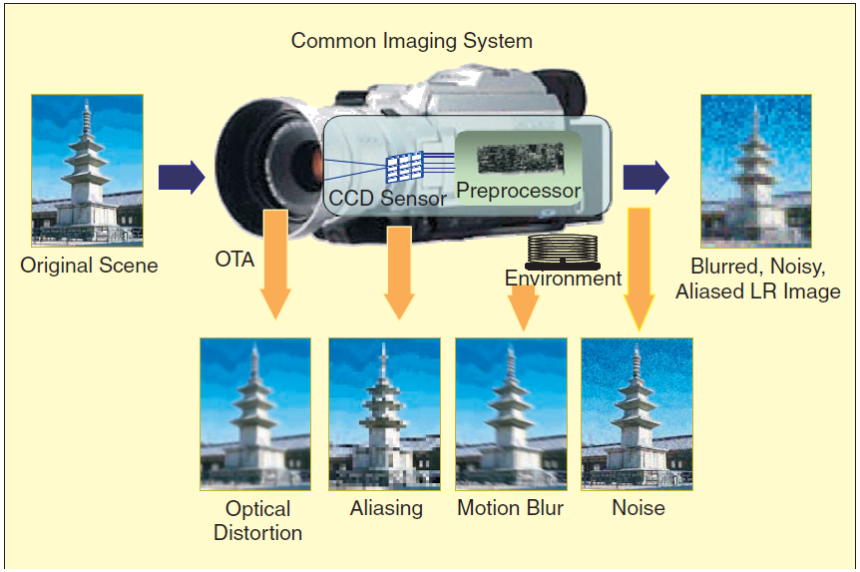

- Superresolution (SR) is the problem of improving the resolution of an image, without introducing artifacts.
- All sensors have a diffraction limit, which restricts resolving power.
- Decreasing pixel size improves resolution, but has the drawback of also decreasing light, leading to shot noise. [12]
- Undersampling leads to aliasing, causing the image to appear blocky.

[12] S. Park, M. Park, and M. Kang. *Super-resolution image reconstruction: a technical overview.* IEEE Signal Processing Magazine 20.3 (2003):21-36.

What is Superresolution?

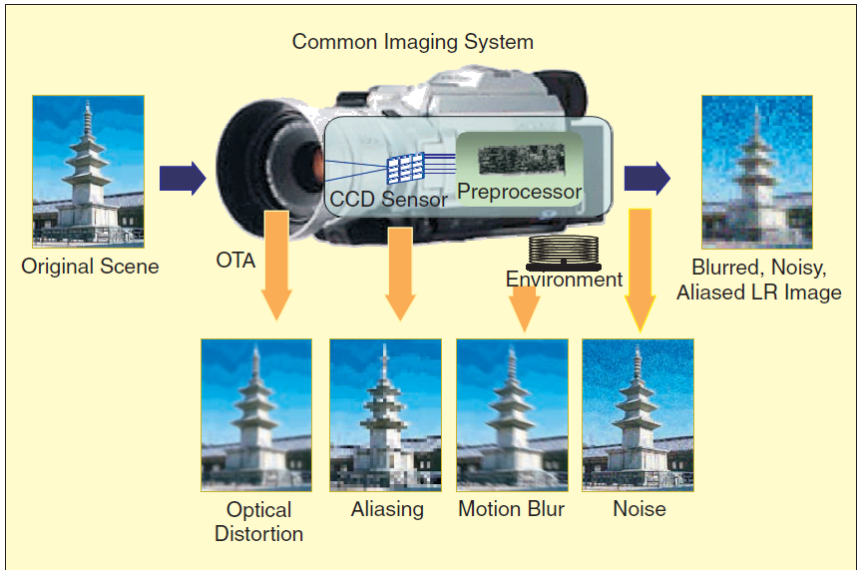

- Superresolution (SR) is the problem of improving the resolution of an image, without introducing artifacts.
- All sensors have a diffraction limit, which restricts resolving power.
- Decreasing pixel size improves resolution, but has the drawback of also decreasing light, leading to shot noise. [12]
- Undersampling leads to aliasing, causing the image to appear blocky.

[12] S. Park, M. Park, and M. Kang. *Super-resolution image reconstruction: a technical overview.* IEEE Signal Processing Magazine 20.3 (2003):21-36.

What is Superresolution?

- Superresolution is often phrased as an image recovery problem. Let f be the observed image and u the image we want to recover. One possible model is [13]

$$f = D(h * u) + n$$

where h is a possibly unknown blur filter, D is a down-sampling operator (which typically introduces aliasing), and n is Gaussian white noise.

- For this presentation, we take the simpler model

$$f = Du$$

and assume D downsamples by a factor of 2.

[13] A. Marquina and S. Osher. *Image super resolution by TV-regularization and Bregman iteration.* J. Sci. Comput. 37 (2008): 367-382.

What is Superresolution?

- Superresolution is often phrased as an image recovery problem. Let f be the observed image and u the image we want to recover. One possible model is [13]

$$f = D(h * u) + n$$

where h is a possibly unknown blur filter, D is a down-sampling operator (which typically introduces aliasing), and n is Gaussian white noise.

- For this presentation, we take the simpler model

$$f = Du$$

and assume D downsamples by a factor of 2.

[13] A. Marquina and S. Osher. *Image super resolution by TV-regularization and Bregman iteration.* J. Sci. Comput. 37 (2008): 367-382.

Superresolution

- The previous problem is ill-posed due to the loss of information in the downsampling process.
- The problem becomes more tractable with additional information.
  - One common technique is to combine multiple low resolution images of the same scene with sub-pixel shifts.
  - Another is to build a dictionary of known high/low resolution pairs from a set of test images. [14]
- We consider the more difficult problem of *single-image superresolution*, where no additional information is available.

[14] W. Freeman, T. Jones, E. Pasztor. *Example-based super-resolution.* Computer Graphics and Applications 22.2 (2002):56-65

Superresolution

- The previous problem is ill-posed due to the loss of information in the downsampling process.
- The problem becomes more tractable with additional information.
  - One common technique is to combine multiple low resolution images of the same scene with sub-pixel shifts.
  - Another is to build a dictionary of known high/low resolution pairs from a set of test images. [14]
- We consider the more difficult problem of *single-image superresolution*, where no additional information is available.

[14] W. Freeman, T. Jones, E. Pasztor. *Example-based super-resolution.* Computer Graphics and Applications 22.2 (2002):56-65

Superresolution

- The previous problem is ill-posed due to the loss of information in the downsampling process.
- The problem becomes more tractable with additional information.
  - One common technique is to combine multiple low resolution images of the same scene with sub-pixel shifts.
  - Another is to build a dictionary of known high/low resolution pairs from a set of test images. [14]
- We consider the more difficult problem of *single-image superresolution*, where no additional information is available.

[14] W. Freeman, T. Jones, E. Pasztor. *Example-based super-resolution.* Computer Graphics and Applications 22.2 (2002):56-65

Single-image Superresolution in the Literature

- New Edge-Directed Interpolation scheme (Li and Orchard) uses estimates of local covariance at the low resolution to interpolate the higher resolution.
- Directional Filtering and Data Fusion (Zhang and Wu) fuses two estimates of a pixel's value through linear minimum mean square-error estimation.
- Soft Decision Adaptive Interpolation (ibid.) uses a $2D$ piecewise autoregressive model, where the model parameters are determined by a soft-decision estimation on groups of pixels.
- Kernel Regression (Takeda, Farsiu, and Milanfar) makes use of non-parametric estimation to denoise and interpolate randomly sampled data.

Superresolution and Harmonic Analysis

- The above single-image superresolution techniques are essentially statistical in nature.
- Harmonic analysis techniques have also been applied to the problem, including:
  - Iterative procedures that impose sparsity in the transform domain (contourlet[15], shearlet[16]).
  - Formations of tight frames from circulant matrices that capture particular directions. [17]
  - Sparse mixing estimation (SME) utilizing orthogonal block matching pursuit on wavelet coefficients. [18]

---

[15] N. Mueller, Y. Lu, and M.N. Do. *Image interpolation using multiscale geometric representations.* In Proc. SPIE Computational Imaging V, pp. 64980A, (2007).

[16] H. Lakshman, W.-Q Lim, H. Schwartz et al. *Image interpolation using shearlet based iterative refinement*. arXiv:1308.1126. (2013).

[17] E.H. Bosch, A. Castrodad, J.S. Cooper, W. Czaja, and J. Dobrosotskaya. *Tight frames for multiscale and multidirectional image analysis.* In SPIE Defense, Security, and Sensing, pp. 875004-875004. International Society for Optics and Photonics. (2013).

[18] S. Mallat and G. Yu. *Super-resolution with sparse mixing estimators*. IEEE Transactions on Image Processing 19.11 (2010): 2889-2900.

Superresolution and Harmonic Analysis

- The above single-image superresolution techniques are essentially statistical in nature.
- Harmonic analysis techniques have also been applied to the problem, including:
  - Iterative procedures that impose sparsity in the transform domain (contourlet[15], shearlet[16]).
  - Formations of tight frames from circulant matrices that capture particular directions. [17]
  - Sparse mixing estimation (SME) utilizing orthogonal block matching pursuit on wavelet coefficients. [18]

---

[15] N. Mueller, Y. Lu, and M.N. Do. *Image interpolation using multiscale geometric representations.* In Proc. SPIE Computational Imaging V, pp. 64980A, (2007).

[16] H. Lakshman, W.-Q Lim, H. Schwartz et al. *Image interpolation using shearlet based iterative refinement*. arXiv:1308.1126. (2013).

[17] E.H. Bosch, A. Castrodad, J.S. Cooper, W. Czaja, and J. Dobrosotskaya. *Tight frames for multiscale and multidirectional image analysis.* In SPIE Defense, Security, and Sensing, pp. 875004-875004. International Society for Optics and Photonics. (2013).

[18] S. Mallat and G. Yu. *Super-resolution with sparse mixing estimators*. IEEE Transactions on Image Processing 19.11 (2010): 2889-2900.

Superresolution Algorithm

1. Let I be the original image/signal. If I has multiple bands, we apply the algorithm to each band separately.
2. Upsample I by bicubic interpolation to obtain I_b.
3. Apply the FFST to I_b. Restrict to a scale of interest.
4. Assign each pixel a dominant local direction based on the direction of the shearlet coefficient of largest magnitude.
5. Pixels whose largest shearlet coefficient is below a threshold T are determined to have no local direction.
6. Pixels within some distance of the border are also assigned to have no local direction.
7. Apply a blur filter of length 5 to I_b in each shearlet direction.
8. Replace each pixel having a dominant local direction with its corresponding “blurred” value.
9. Output the superresolved image.

Details of Superresolution Algorithm

- If I is an $M \times N$ image with $max\{M, N\} \geq 128$, we can obtain a decomposition of I_b into 4 scales with 2^{j+1} directions at scale j.
- We choose $j = 3$ as the scale of interest, since it will contain the edges and few textures.
- The threshold T is typically taken to be about 0.04 for normalized images.
- The FFST gives spurious information near the border, so this information is discarded.

Details of Superresolution Algorithm

- If I is an $M \times N$ image with $max\{M, N\} \geq 128$, we can obtain a decomposition of I_b into 4 scales with 2^{j+1} directions at scale j.
- We choose $j = 3$ as the scale of interest, since it will contain the edges and few textures.
- The threshold T is typically taken to be about 0.04 for normalized images.
- The FFST gives spurious information near the border, so this information is discarded.

Details of Superresolution Algorithm

- If I is an $M \times N$ image with $max\{M, N\} \geq 128$, we can obtain a decomposition of I_b into 4 scales with 2^{j+1} directions at scale j.
- We choose $j = 3$ as the scale of interest, since it will contain the edges and few textures.
- The threshold T is typically taken to be about 0.04 for normalized images.
- The FFST gives spurious information near the border, so this information is discarded.

Details of Superresolution Algorithm

- If I is an $M \times N$ image with $max\{M, N\} \geq 128$, we can obtain a decomposition of I_b into 4 scales with 2^{j+1} directions at scale j.
- We choose $j = 3$ as the scale of interest, since it will contain the edges and few textures.
- The threshold T is typically taken to be about 0.04 for normalized images.
- The FFST gives spurious information near the border, so this information is discarded.

Experiments

- We tested our algorithm on a color orthophoto of an urban area in Zeebruges, Belgium with spatial resolution 5-cm. [19]
- We extracted a 512×512 subset of the image and then downsampled by a factor of 2.

Figure: Original image (left) and downsampled image (right)

[19] 2015 IEEE GRSS Data Fusion Contest. http://www.grss-ieee.org/community/technical-committees/data-fusion/.

Results of Experiments

- The downsampled image was then superresolved with bicubic convolution, SME, and our algorithm.
- Here, we zoom in on a 100 $\times$ 100 subset to observe the fine details.

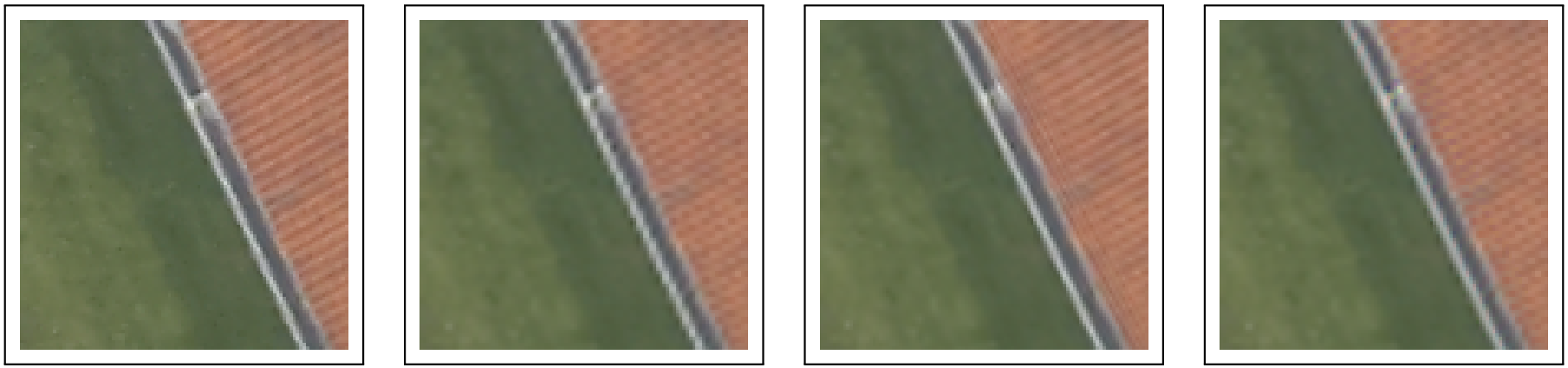

(a) Original (b) Bicubic (c) SME (d) Shearlet-based

Figure: A comparison of the three methods on a zoomed-in area of the image.

Comparison of Methods

- Our algorithm is quite fast.
  - We performed SME and our algorithm on each channel of the RGB image.
  - Computations were performed on a MacBook Pro with a 2.6 GHz Intel Core i5 processor and 16 GB of RAM.
  - Timings: bicubic (instant), SME (705 s), our algorithm (3 s).
- Bicubic preserves jagged edges caused by aliasing. SME and our algorithm smooth the edges.
- SME leads to sharper edges and fewer blurred textures than our algorithm.
- However, SME causes some undesirable artifacts, which appear as thin lines in the roof.

Comparison of Methods

- Our algorithm is quite fast.
  - We performed SME and our algorithm on each channel of the RGB image.
  - Computations were performed on a MacBook Pro with a 2.6 GHz Intel Core i5 processor and 16 GB of RAM.
  - Timings: bicubic (instant), SME (705 s), our algorithm (3 s).
- Bicubic preserves jagged edges caused by aliasing. SME and our algorithm smooth the edges.
- SME leads to sharper edges and fewer blurred textures than our algorithm.
- However, SME causes some undesirable artifacts, which appear as thin lines in the roof.

Comparison of Methods

- Our algorithm is quite fast.
  - We performed SME and our algorithm on each channel of the RGB image.
  - Computations were performed on a MacBook Pro with a 2.6 GHz Intel Core i5 processor and 16 GB of RAM.
  - Timings: bicubic (instant), SME (705 s), our algorithm (3 s).
- Bicubic preserves jagged edges caused by aliasing. SME and our algorithm smooth the edges.
- SME leads to sharper edges and fewer blurred textures than our algorithm.
- However, SME causes some undesirable artifacts, which appear as thin lines in the roof.

Comparison of Methods

- Our algorithm is quite fast.
  - We performed SME and our algorithm on each channel of the RGB image.
  - Computations were performed on a MacBook Pro with a 2.6 GHz Intel Core i5 processor and 16 GB of RAM.
  - Timings: bicubic (instant), SME (705 s), our algorithm (3 s).
- Bicubic preserves jagged edges caused by aliasing. SME and our algorithm smooth the edges.
- SME leads to sharper edges and fewer blurred textures than our algorithm.
- However, SME causes some undesirable artifacts, which appear as thin lines in the roof.

Summary and Future Directions

- In general, anisotropic harmonic analysis provides a powerful set of techniques for superresolution in terms of visual quality.
- One of the greatest challenges for our algorithm is superresolving images with many textures without oversmoothing.
- In future work, we would like to find a method for filtering out the textures so as to only smooth the edges.
- In addition, we would like to consider more sophisticated ways of improving edges beyond motion blurring, which tends to decrease image sharpness.
- We will further study Mallat's SME method to determine if shearlets can offer any improvements.

Summary and Future Directions

- In general, anisotropic harmonic analysis provides a powerful set of techniques for superresolution in terms of visual quality.
- One of the greatest challenges for our algorithm is superresolving images with many textures without oversmoothing.
- In future work, we would like to find a method for filtering out the textures so as to only smooth the edges.
- In addition, we would like to consider more sophisticated ways of improving edges beyond motion blurring, which tends to decrease image sharpness.
- We will further study Mallat's SME method to determine if shearlets can offer any improvements.

Summary and Future Directions

- In general, anisotropic harmonic analysis provides a powerful set of techniques for superresolution in terms of visual quality.
- One of the greatest challenges for our algorithm is superresolving images with many textures without oversmoothing.
- In future work, we would like to find a method for filtering out the textures so as to only smooth the edges.
- In addition, we would like to consider more sophisticated ways of improving edges beyond motion blurring, which tends to decrease image sharpness.
- We will further study Mallat's SME method to determine if shearlets can offer any improvements.

Summary and Future Directions

- In general, anisotropic harmonic analysis provides a powerful set of techniques for superresolution in terms of visual quality.
- One of the greatest challenges for our algorithm is superresolving images with many textures without oversmoothing.
- In future work, we would like to find a method for filtering out the textures so as to only smooth the edges.
- In addition, we would like to consider more sophisticated ways of improving edges beyond motion blurring, which tends to decrease image sharpness.
- We will further study Mallat's SME method to determine if shearlets can offer any improvements.

Summary and Future Directions

- In general, anisotropic harmonic analysis provides a powerful set of techniques for superresolution in terms of visual quality.
- One of the greatest challenges for our algorithm is superresolving images with many textures without oversmoothing.
- In future work, we would like to find a method for filtering out the textures so as to only smooth the edges.
- In addition, we would like to consider more sophisticated ways of improving edges beyond motion blurring, which tends to decrease image sharpness.
- We will further study Mallat's SME method to determine if shearlets can offer any improvements.

A Shearlet Application to LIDAR

What is LIDAR?

- LIDAR (Light Detection and Ranging) is a remote-sensing technique that uses lasers to acquire elevation data.
- A collection vehicle (plane, helicopter, car) emits light, which reflects off the ground (or a structure on the ground) and back to a sensor.
- By analyzing the time of return, elevation data can be obtained.
- Multiple returns occur when light strikes semi-permeable object, such as trees.
- Intensities may also be collected; they measure material reflectivity.
- Recently, LIDAR has become an indispensable component of self-driving cars.

What is LIDAR?

- LIDAR (Light Detection and Ranging) is a remote-sensing technique that uses lasers to acquire elevation data.
- A collection vehicle (plane, helicopter, car) emits light, which reflects off the ground (or a structure on the ground) and back to a sensor.
- By analyzing the time of return, elevation data can be obtained.
- Multiple returns occur when light strikes semi-permeable object, such as trees.
- Intensities may also be collected; they measure material reflectivity.
- Recently, LIDAR has become an indispensable component of self-driving cars.

What is LIDAR?

- LIDAR (Light Detection and Ranging) is a remote-sensing technique that uses lasers to acquire elevation data.
- A collection vehicle (plane, helicopter, car) emits light, which reflects off the ground (or a structure on the ground) and back to a sensor.
- By analyzing the time of return, elevation data can be obtained.
- Multiple returns occur when light strikes semi-permeable object, such as trees.
- Intensities may also be collected; they measure material reflectivity.
- Recently, LIDAR has become an indispensable component of self-driving cars.

What is LIDAR?

- LIDAR (Light Detection and Ranging) is a remote-sensing technique that uses lasers to acquire elevation data.
- A collection vehicle (plane, helicopter, car) emits light, which reflects off the ground (or a structure on the ground) and back to a sensor.
- By analyzing the time of return, elevation data can be obtained.
- Multiple returns occur when light strikes semi-permeable object, such as trees.
- Intensities may also be collected; they measure material reflectivity.
- Recently, LIDAR has become an indispensable component of self-driving cars.

What is LIDAR?

- LIDAR (Light Detection and Ranging) is a remote-sensing technique that uses lasers to acquire elevation data.
- A collection vehicle (plane, helicopter, car) emits light, which reflects off the ground (or a structure on the ground) and back to a sensor.
- By analyzing the time of return, elevation data can be obtained.
- Multiple returns occur when light strikes semi-permeable object, such as trees.
- Intensities may also be collected; they measure material reflectivity.
- Recently, LIDAR has become an indispensable component of self-driving cars.

What is LIDAR?

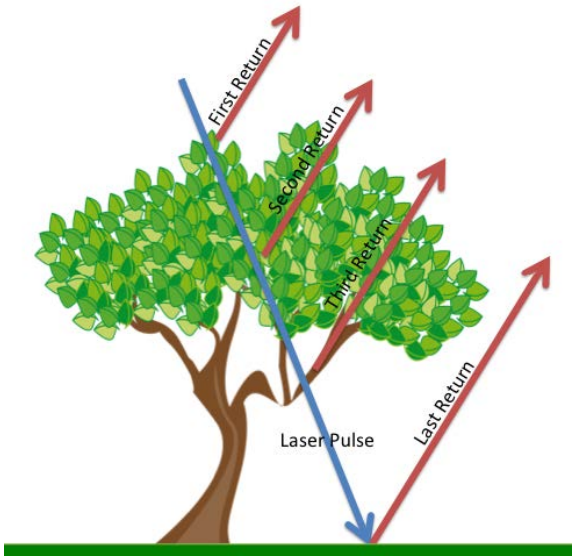

Illustration of LIDAR returns[20] (left) and Google prototype with LIDAR system on roof[21] (right).

[20] T. Doster. *Harmonic Analysis Inspired Data Fusion for Applications in Remote Sensing*. PhD thesis. (2014).

[21] S. Gibbs. *Google's self-driving car: How does it work and when can we drive one?* The Guardian. (2014).

Description of the Problem

- We have gridded first-return LIDAR data of rural scenes without intensities.
- We would like to detect quasilinear structures (roads, ditches).
- Challenges:
  - Trees dominate scenes and need to be filtered out.
  - Roads and ditches do not stand out much from their surroundings in LIDAR.
  - Roads are *weak edges* and do not persist across scales.
- To meet these challenges, we need scale and directionality information.
  - By choosing the appropriate scale, we can focus on the weak edges.
  - By including directionality, we can seek out locally linear objects.
- We develop a shearlet-based algorithm for feature detection.

Description of the Problem

- We have gridded first-return LIDAR data of rural scenes without intensities.
- We would like to detect quasilinear structures (roads, ditches).
- Challenges:
  - Trees dominate scenes and need to be filtered out.
  - Roads and ditches do not stand out much from their surroundings in LIDAR.
  - Roads are *weak edges* and do not persist across scales.
- To meet these challenges, we need scale and directionality information.
  - By choosing the appropriate scale, we can focus on the weak edges.
  - By including directionality, we can seek out locally linear objects.
- We develop a shearlet-based algorithm for feature detection.

Description of the Problem

- We have gridded first-return LIDAR data of rural scenes without intensities.
- We would like to detect quasilinear structures (roads, ditches).
- Challenges:
  - Trees dominate scenes and need to be filtered out.
  - Roads and ditches do not stand out much from their surroundings in LIDAR.
  - Roads are *weak edges* and do not persist across scales.
- To meet these challenges, we need scale and directionality information.
  - By choosing the appropriate scale, we can focus on the weak edges.
  - By including directionality, we can seek out locally linear objects.
- We develop a shearlet-based algorithm for feature detection.

Description of the Problem

- We have gridded first-return LIDAR data of rural scenes without intensities.
- We would like to detect quasilinear structures (roads, ditches).
- Challenges:
  - Trees dominate scenes and need to be filtered out.
  - Roads and ditches do not stand out much from their surroundings in LIDAR.
  - Roads are *weak edges* and do not persist across scales.
- To meet these challenges, we need scale and directionality information.
  - By choosing the appropriate scale, we can focus on the weak edges.
  - By including directionality, we can seek out locally linear objects.
- We develop a shearlet-based algorithm for feature detection.

Description of the Problem

- We have gridded first-return LIDAR data of rural scenes without intensities.
- We would like to detect quasilinear structures (roads, ditches).
- Challenges:
  - Trees dominate scenes and need to be filtered out.
  - Roads and ditches do not stand out much from their surroundings in LIDAR.
  - Roads are *weak edges* and do not persist across scales.
- To meet these challenges, we need scale and directionality information.
  - By choosing the appropriate scale, we can focus on the weak edges.
  - By including directionality, we can seek out locally linear objects.
- We develop a shearlet-based algorithm for feature detection.

The Mohawk Ditch Scene

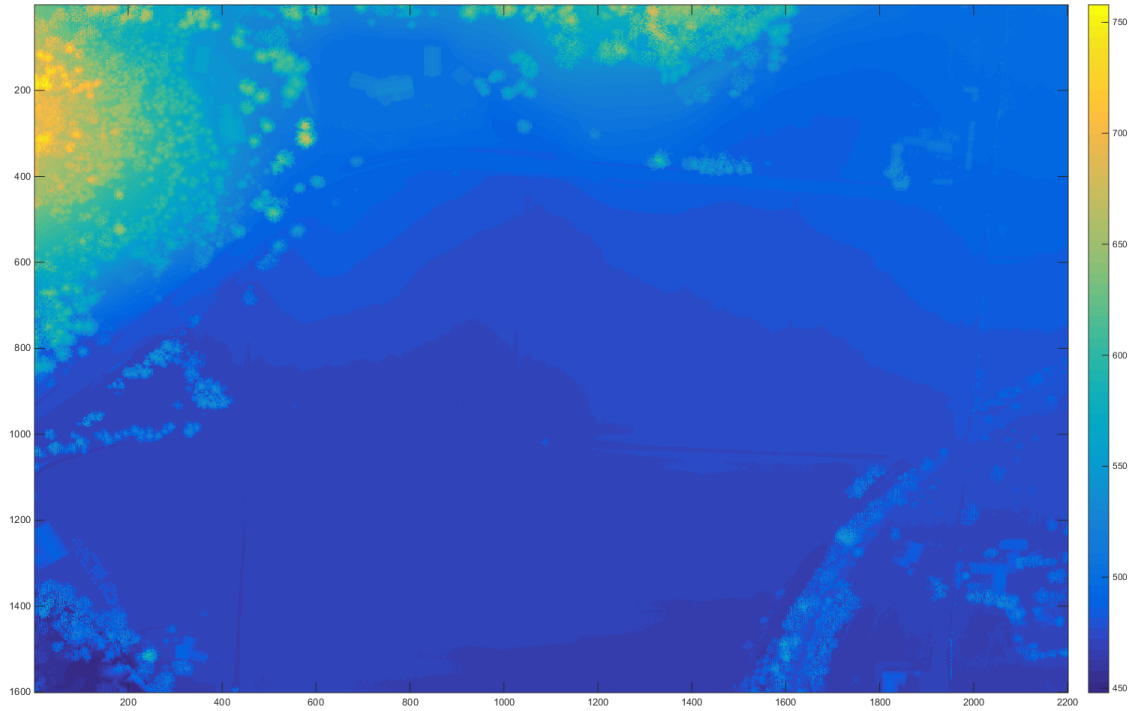

Figure: Original gridded LIDAR data, courtesy of the Army Research Labs.

The Mohawk Ditch Scene

- Trees dominate the scene and there are some hints of roads.
- A good way to visualize the information content in such a scene is to apply a standard deviation filter and take the logarithm (logstd).

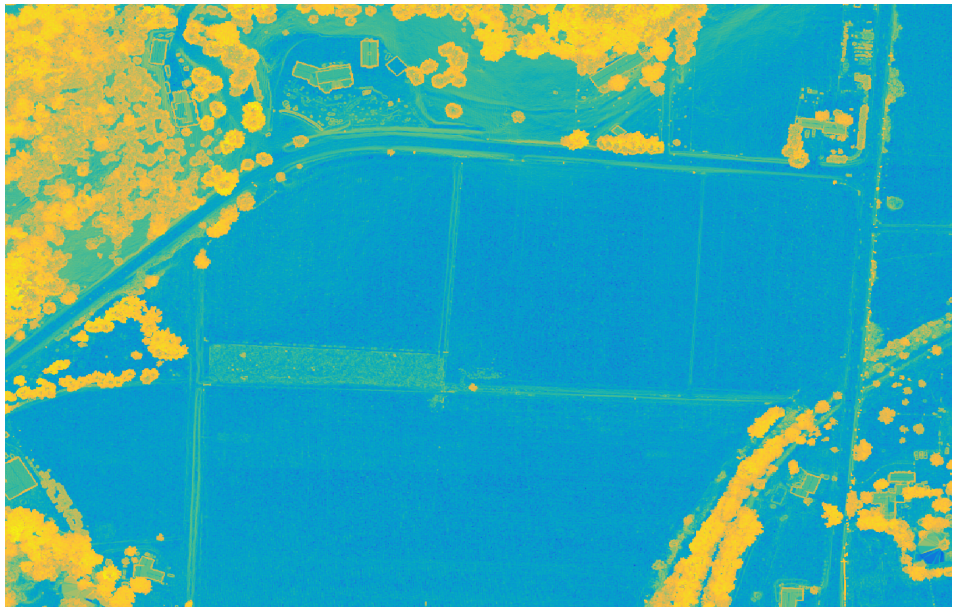

Figure: Log of the standard deviation-filtered data.

The Mohawk Ditch Scene

- Large shearlet coefficients at a point mean high local directionality.
- Thresholding from below gives directional features, while thresholding from above removes trees.
- We perform the shearlet transform with four scales. The features of interest are in scale 3.

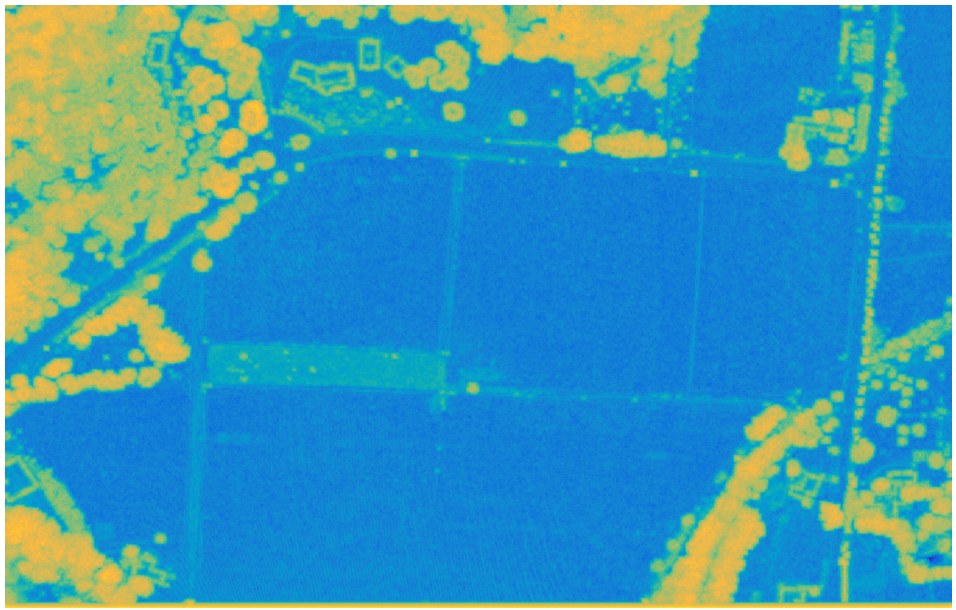

Figure: Log of sum of the shearlet coefficient magnitudes at scale 3.

Is Thresholding Shearlet Coefficients Enough?

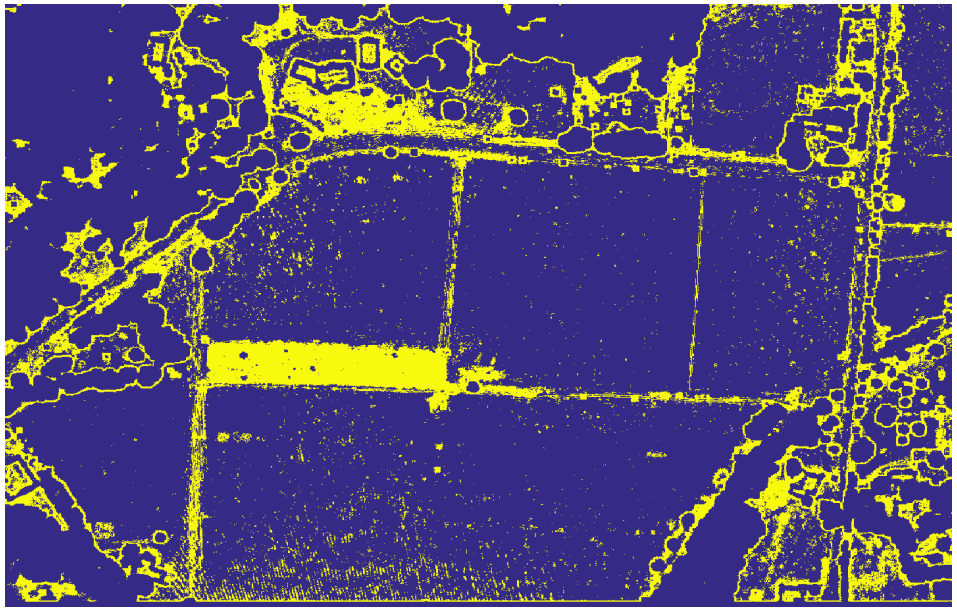

Figure: Locations where the sum of shearlet coefficients is between 0.12 and 1 at scale 3.

- We capture locations of ditches and roads, but also edges of trees.
- The large shearlet coefficients of the trees cause a bleeding effect, so tree edges cannot be filtered out.
- We need to find a better way to use the information.

Is Thresholding Shearlet Coefficients Enough?

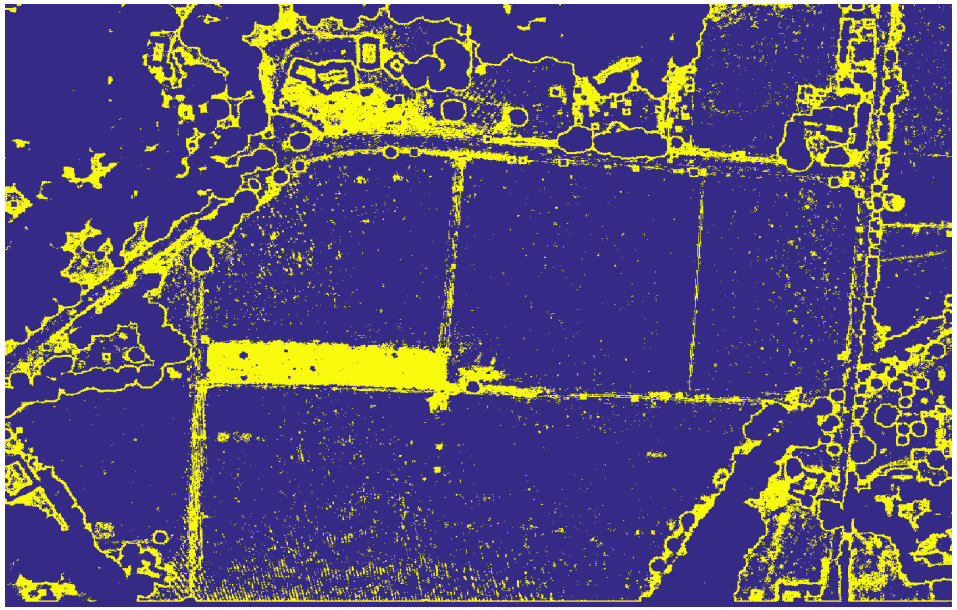

Figure: Locations where the sum of shearlet coefficients is between 0.12 and 1 at scale 3.

- We capture locations of ditches and roads, but also edges of trees.
- The large shearlet coefficients of the trees cause a bleeding effect, so tree edges cannot be filtered out.
- We need to find a better way to use the information.

Detection Algorithm

1. Let A be the original LIDAR image. Define $B := A - \min(A)$.
2. Compute the FFST of B. Restrict to a scale of interest.
3. Specify four thresholding parameters: *loglow*, *loghi*, *elevhi*, and *shearhi*. These parameters are thresholds on the logstd, the elevation from the minimum point, and the shearlet coefficient, respectively.
4. Each point that satisfies the standard deviation and elevation thresholds are candidates for the edge points we are interested in. For each of the points, record the number of directions whose shearlet coefficient has magnitude below *shearhi*.
5. Remove the points that have small shearlet coefficients in all directions.
6. Apply a median filter determined by a vector $mfilt = [m, n]$, where m and n are odd.
7. Output the resulting image.

Details of the Detection Algorithm

- Since the logstd allows us to see what is in the scene, it makes sense to threshold by it.
- Thresholding the elevation from above with respect to the lowest point will remove trees, at least for flat terrain.
- For directional features, the shearlet coefficient will ideally be large in only one direction. We relax this constraint by allowing it to be large in other directions, but consider more small coefficients (determined by *shearhi*) to be better evidence of detecting a structure of interest.
- The median filter is needed as post-processing to remove isolated pixels.
- The result will be an image of pixels that satisfy the thresholds. Each pixel will have value given by the number of small shearlet directions.

Details of the Detection Algorithm

- Since the logstd allows us to see what is in the scene, it makes sense to threshold by it.
- Thresholding the elevation from above with respect to the lowest point will remove trees, at least for flat terrain.
- For directional features, the shearlet coefficient will ideally be large in only one direction. We relax this constraint by allowing it to be large in other directions, but consider more small coefficients (determined by *shearhi*) to be better evidence of detecting a structure of interest.
- The median filter is needed as post-processing to remove isolated pixels.
- The result will be an image of pixels that satisfy the thresholds. Each pixel will have value given by the number of small shearlet directions.

Details of the Detection Algorithm

- Since the logstd allows us to see what is in the scene, it makes sense to threshold by it.
- Thresholding the elevation from above with respect to the lowest point will remove trees, at least for flat terrain.
- For directional features, the shearlet coefficient will ideally be large in only one direction. We relax this constraint by allowing it to be large in other directions, but consider more small coefficients (determined by *shearhi*) to be better evidence of detecting a structure of interest.
- The median filter is needed as post-processing to remove isolated pixels.
- The result will be an image of pixels that satisfy the thresholds. Each pixel will have value given by the number of small shearlet directions.

Details of the Detection Algorithm

- Since the logstd allows us to see what is in the scene, it makes sense to threshold by it.
- Thresholding the elevation from above with respect to the lowest point will remove trees, at least for flat terrain.
- For directional features, the shearlet coefficient will ideally be large in only one direction. We relax this constraint by allowing it to be large in other directions, but consider more small coefficients (determined by *shearhi*) to be better evidence of detecting a structure of interest.
- The median filter is needed as post-processing to remove isolated pixels.
- The result will be an image of pixels that satisfy the thresholds. Each pixel will have value given by the number of small shearlet directions.

Details of the Detection Algorithm

- Since the logstd allows us to see what is in the scene, it makes sense to threshold by it.
- Thresholding the elevation from above with respect to the lowest point will remove trees, at least for flat terrain.
- For directional features, the shearlet coefficient will ideally be large in only one direction. We relax this constraint by allowing it to be large in other directions, but consider more small coefficients (determined by *shearhi*) to be better evidence of detecting a structure of interest.
- The median filter is needed as post-processing to remove isolated pixels.
- The result will be an image of pixels that satisfy the thresholds. Each pixel will have value given by the number of small shearlet directions.

Results

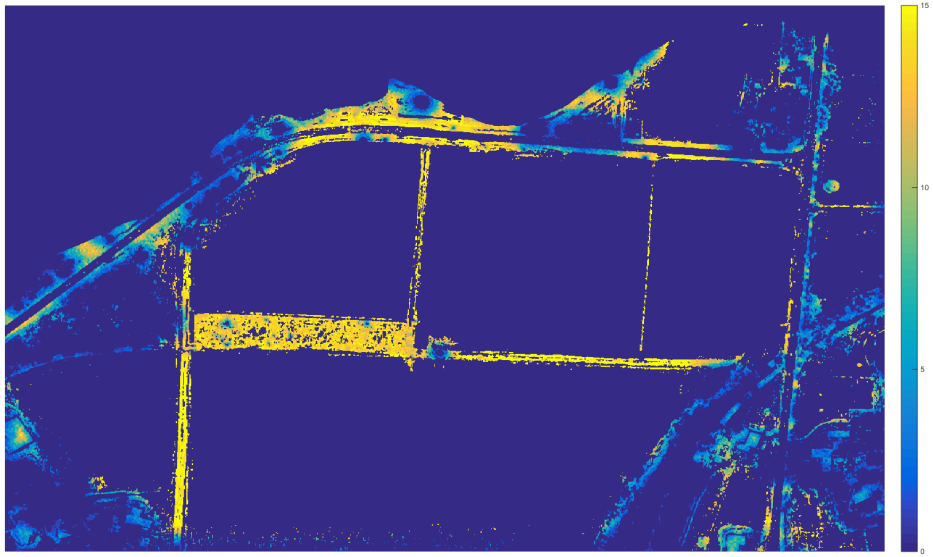

Figure: Results of algorithm with $loglow = -2.4$, $loghi = 0$, $shearhi = 0.1$, $elevhi = 50$, and $mfilt = [5, 3]$. Yellow and orange pixels are strongly directional, green is moderately directional, light blue is weakly directional, dark blue is non-directional.

Results

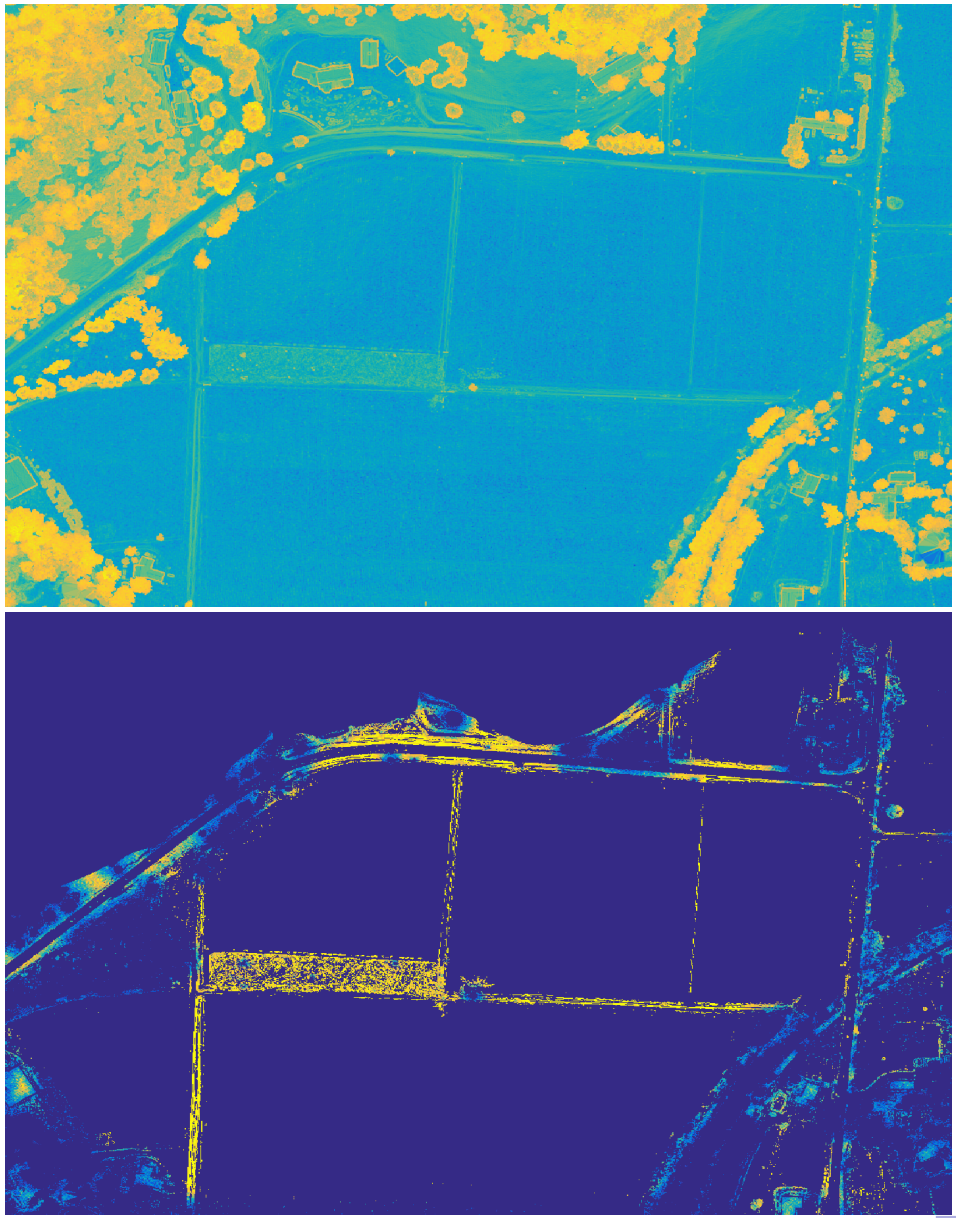

Results

- Trees have almost entirely been filtered out.
- As hypothesized, points with many small shearlet coefficients do tend to belong to roads and ditches.
- It was important to keep weakly directional points to fill in large gaps.
- Some gaps are unavoidable, either due to exceptionally thin edges or tree-covered roads.
- False positives tend to be either roofs of buildings or regions between trees.

Results

- Trees have almost entirely been filtered out.
- As hypothesized, points with many small shearlet coefficients do tend to belong to roads and ditches.
- It was important to keep weakly directional points to fill in large gaps.
- Some gaps are unavoidable, either due to exceptionally thin edges or tree-covered roads.
- False positives tend to be either roofs of buildings or regions between trees.

Results

- Trees have almost entirely been filtered out.
- As hypothesized, points with many small shearlet coefficients do tend to belong to roads and ditches.
- It was important to keep weakly directional points to fill in large gaps.
- Some gaps are unavoidable, either due to exceptionally thin edges or tree-covered roads.
- False positives tend to be either roofs of buildings or regions between trees.

Results

- Trees have almost entirely been filtered out.
- As hypothesized, points with many small shearlet coefficients do tend to belong to roads and ditches.
- It was important to keep weakly directional points to fill in large gaps.
- Some gaps are unavoidable, either due to exceptionally thin edges or tree-covered roads.
- False positives tend to be either roofs of buildings or regions between trees.

Results

- Trees have almost entirely been filtered out.
- As hypothesized, points with many small shearlet coefficients do tend to belong to roads and ditches.
- It was important to keep weakly directional points to fill in large gaps.
- Some gaps are unavoidable, either due to exceptionally thin edges or tree-covered roads.
- False positives tend to be either roofs of buildings or regions between trees.

A More Difficult Example: Gainsville Track

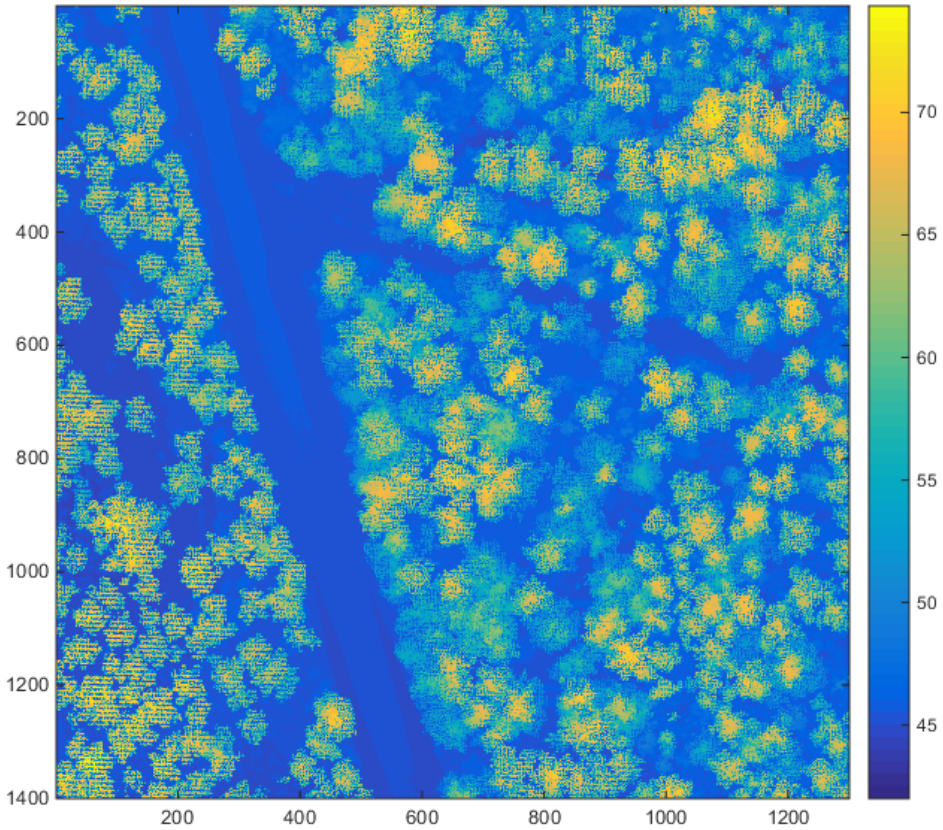

Figure: Original LIDAR data.

Gainsville Track

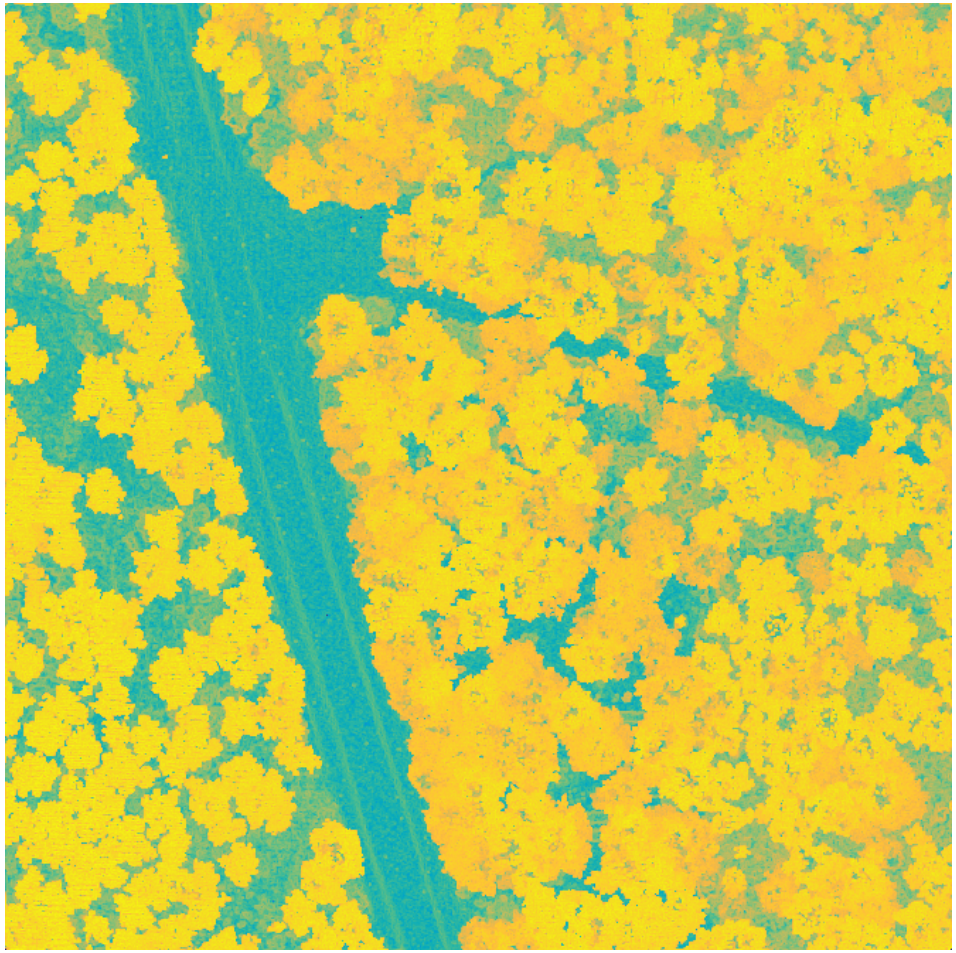

Figure: Logstd of the Gainsville track scene. Note the barely detectable dirt road.

Results

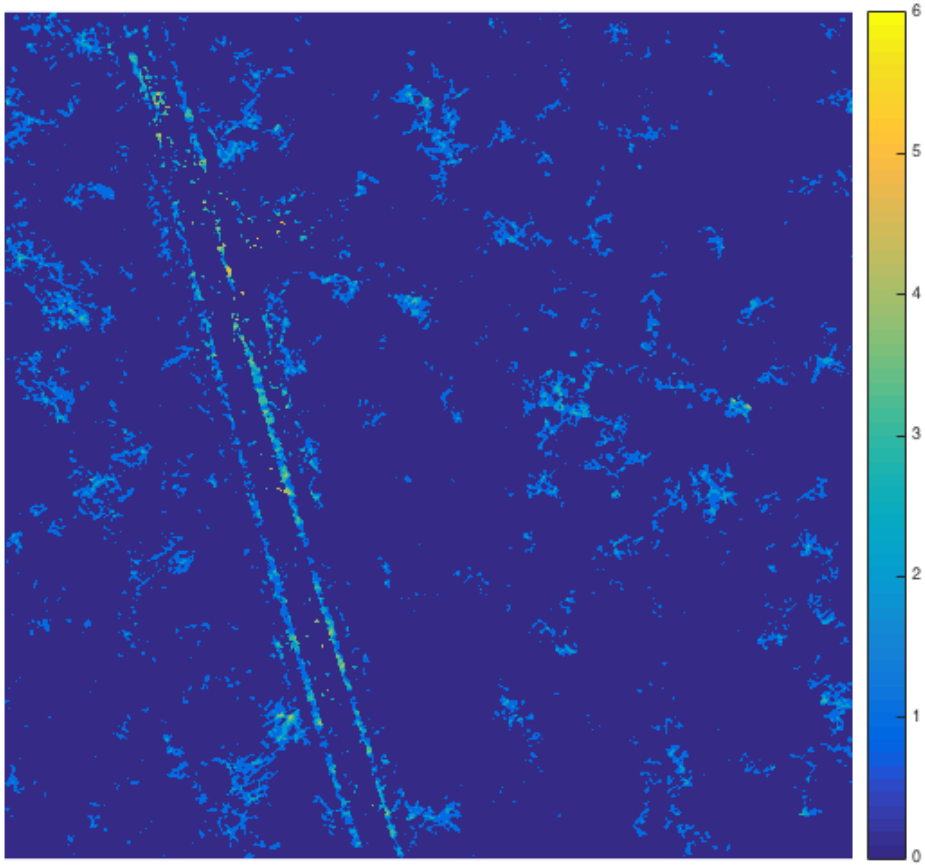

Figure: Results of the algorithm on the Gainsville track scene with $loglow = -4$, $loghi = 0$, $shearhi = 0.1$, $elevhi = 5$, and $mfilt = [5, 5]$. Scale 2 is used here, so there can be at most 7 weak directions.

Results

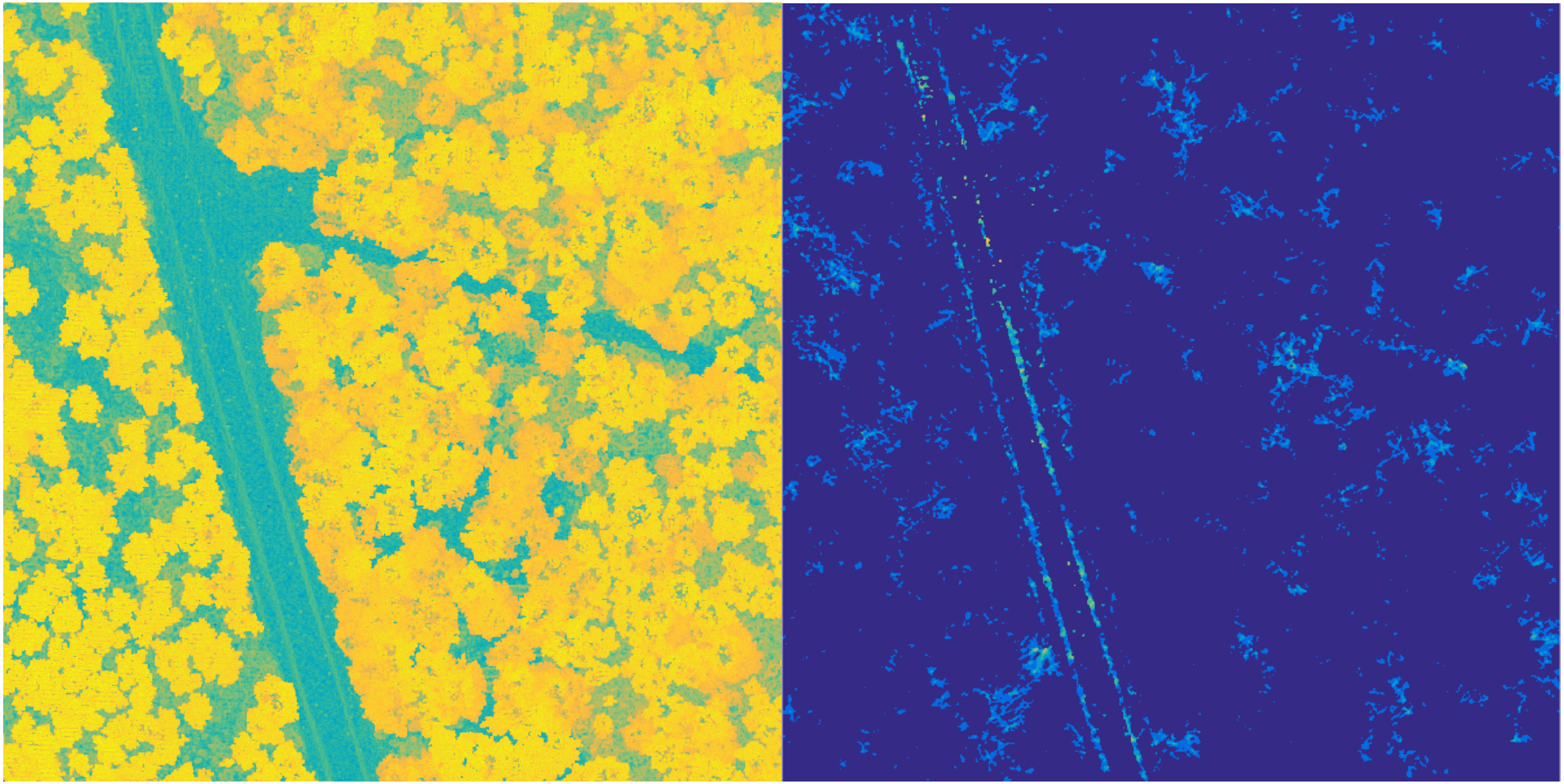

Results

- The detected road contains all strongly directional points.
- There are breaks in the detected road, but in fact they are in the original data.
- Regions between trees are also detected as before.
- We need global shape analysis to detect and remove these regions.

Results

- The detected road contains all strongly directional points.
- There are breaks in the detected road, but in fact they are in the original data.
- Regions between trees are also detected as before.
- We need global shape analysis to detect and remove these regions.

Results

- The detected road contains all strongly directional points.
- There are breaks in the detected road, but in fact they are in the original data.
- Regions between trees are also detected as before.
- We need global shape analysis to detect and remove these regions.

Results

- The detected road contains all strongly directional points.
- There are breaks in the detected road, but in fact they are in the original data.
- Regions between trees are also detected as before.
- We need global shape analysis to detect and remove these regions.

The Hough Transform

- The Hough transform can be used to detect straight lines in a binary image.
- Essentially, it counts the number of points that pass through various lines.
- Each line is parametrized as $\rho = x\cos(\theta) + y\sin(\theta)$.
- It can be thought of as a discrete version of the Radon transform.

The Hough Transform

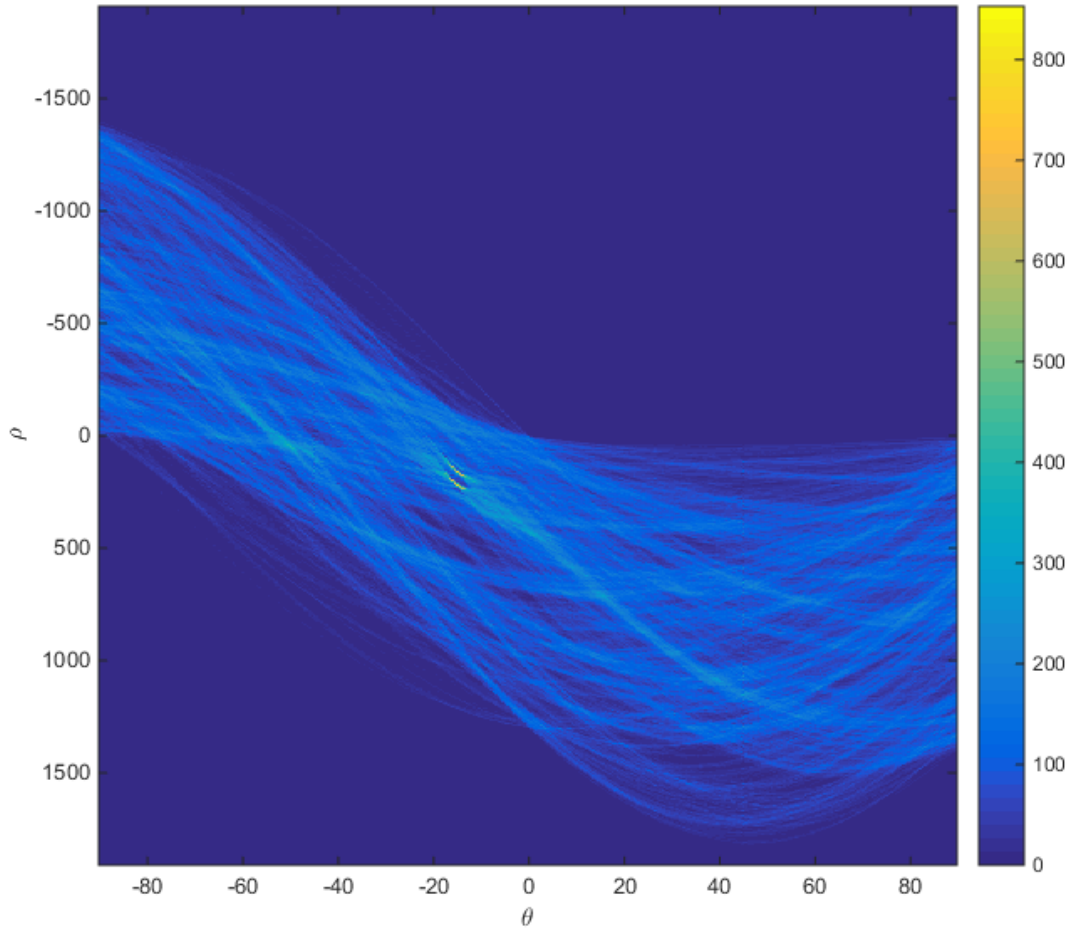

Figure: The Hough transform of the binary-converted output.

The Hough Transform

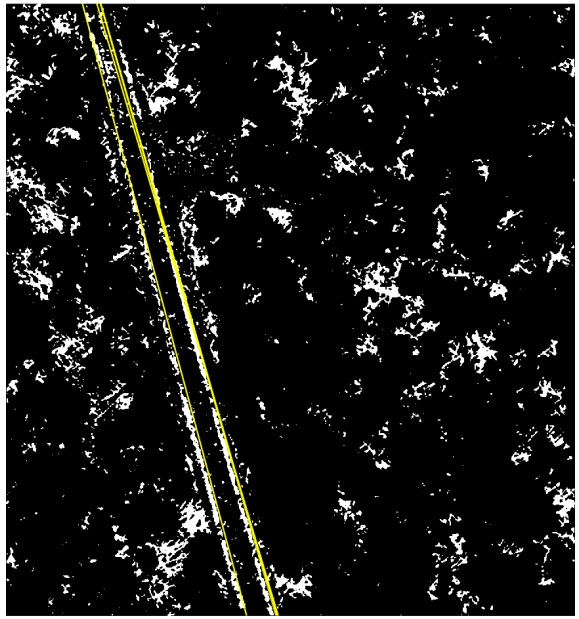

Figure: Plot of the ten most significant lines as determined by the Hough transform, superimposed on the binary-converted results of the algorithm.

- Three distinct lines were detected.
- Averaging the values corresponding to each line, we obtain that the lines are described by $(\theta, \rho) = (-15.5, 200), (-15, 209.5), (-14, 170)$.

The Hough Transform

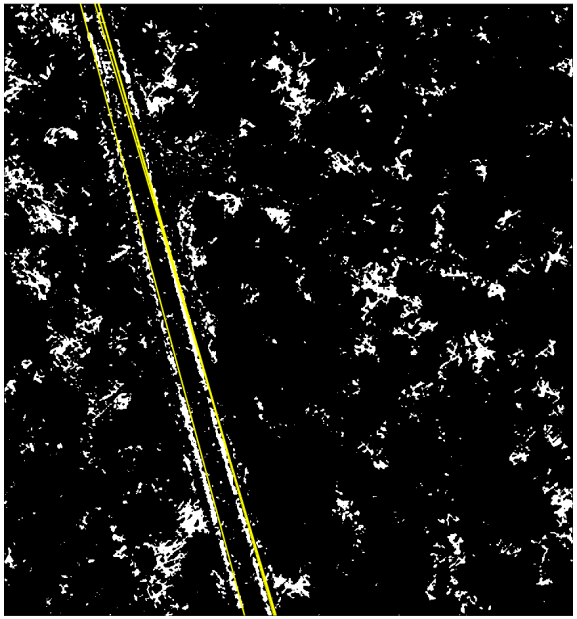

Figure: Plot of the ten most significant lines as determined by the Hough transform, superimposed on the binary-converted results of the algorithm.

- Three distinct lines were detected.
- Averaging the values corresponding to each line, we obtain that the lines are described by $(\theta, \rho) = (-15.5, 200), (-15, 209.5), (-14, 170)$.

Conclusions and Future Work

- We were able to detect roads and ditches by local variance and directionality.
- We needed to relax the condition of only one shearlet coefficient being large.
- The algorithm produces false positives for areas between trees, tops of buildings, and bushes.
- Global shape analysis is needed to filter out these features.
- We would also like to incorporate information from the entire LIDAR point cloud.
  - Multiple returns would allow us to detect roads beneath trees.
  - Intensities may allow us to distinguish the tops of buildings.

Conclusions and Future Work

- We were able to detect roads and ditches by local variance and directionality.
- We needed to relax the condition of only one shearlet coefficient being large.
- The algorithm produces false positives for areas between trees, tops of buildings, and bushes.
- Global shape analysis is needed to filter out these features.
- We would also like to incorporate information from the entire LIDAR point cloud.
  - Multiple returns would allow us to detect roads beneath trees.
  - Intensities may allow us to distinguish the tops of buildings.

Conclusions and Future Work

- We were able to detect roads and ditches by local variance and directionality.
- We needed to relax the condition of only one shearlet coefficient being large.
- The algorithm produces false positives for areas between trees, tops of buildings, and bushes.
- Global shape analysis is needed to filter out these features.
- We would also like to incorporate information from the entire LIDAR point cloud.
  - Multiple returns would allow us to detect roads beneath trees.
  - Intensities may allow us to distinguish the tops of buildings.

Conclusions and Future Work

- We were able to detect roads and ditches by local variance and directionality.
- We needed to relax the condition of only one shearlet coefficient being large.
- The algorithm produces false positives for areas between trees, tops of buildings, and bushes.
- Global shape analysis is needed to filter out these features.
- We would also like to incorporate information from the entire LIDAR point cloud.
  - Multiple returns would allow us to detect roads beneath trees.
  - Intensities may allow us to distinguish the tops of buildings.

Conclusions and Future Work

- We were able to detect roads and ditches by local variance and directionality.
- We needed to relax the condition of only one shearlet coefficient being large.
- The algorithm produces false positives for areas between trees, tops of buildings, and bushes.
- Global shape analysis is needed to filter out these features.
- We would also like to incorporate information from the entire LIDAR point cloud.
  - Multiple returns would allow us to detect roads beneath trees.
  - Intensities may allow us to distinguish the tops of buildings.